ETHZ-IMP PR-93-1
February 1993

49

PRECISION MEASUREMENTS IN MUON AND TAU DECAYS *

W. Fetscher and H.-J. Gerber

Institut für Mittelenergiephysik (IMP), ETH Zürich,
CH-5232 Villigen, Switzerland

Zurich, ETH

---

*To be published in *Precision Tests of the Standard Electroweak Model*, ed. P. Langacker, World Scientific, Singapore, 1993.

Institut für
Mittelenergiephysik (IMP)
ETH Zürich

CH-5232 Villigen
Switzerland

1. Introduction

The standard model [1, 2, 3] introduces the $V-A$ form of the charged leptonic weak interaction *by construction.* It has been shown recently that $V-A$ *follows* from a small set of experiments [4]. We will present the corresponding methods and discuss the room left open by the experimental errors for interactions other than $V-A$. For muons, all of these experiments have been performed.

The most general, derivative-free, lepton-number conserving four-fermion interaction [5] contains ten complex coupling constants which represent nineteen free parameters to be determined by experiment. Based on fields with definite chiralities and using the freedom of the Fierz transformations, a set of coupling constants may be chosen such that the $V-A$ interaction corresponds to *one single constant* only [6, 7]. The experimental proof of $V-A$ then consists in the construction of measurable quantities which evaluate the remaining eighteen constants to be zero [4]. To achieve this, use is made of the general fact (pointed out in Ref. [8]) that a null-result for a sum of positive semi-definite terms requires each term to be zero.

For the muon decay interaction, the ten complex planes of Fig. 2.2 represent a lower limit for $V-A$ and upper limits for the nine remaining couplings.

If lepton-number conservation is not assumed, other decays like $\mu \to e\gamma$ become possible, which open windows to new physics. Experiments looking for such forbidden decays have been driven to a level of 10^{-13} for the muon and 10^{-5} for the tau (see reviews [9] and [10], respectively). The lepton-number non-conserving four-fermion interaction has been studied in detail [11, 12]. The authors of Ref. [12] arrive at the interesting result that it is not possible, even in principle, to test lepton-number conservation in muon decay if the final neutrinos are massless and are not observed.

In this review we wish to present *examples* of typical thoughts which inspired experiments and their analysis and which led to the present knowledge of the Lorentz structure of the charged leptonic weak interaction.

Since there exist complete reviews on experimental results [13], on the future of muon physics in general [14], with emphasis on rare and forbidden processes [9], on theoretical [15, 16, 17] and historical [18] aspects, we allow ourselves to be complementary rather than to aim at completeness.

2. Muon Decay

2.1. Hamiltonian

The three leptonic decays $\mu^+ \to \bar{\nu}_\mu e^+ \nu_e$, $\tau^+ \to \bar{\nu}_\tau \mu^+ \nu_\mu$ and $\tau^+ \to \bar{\nu}_\tau e^+ \nu_e$, as well as their charge conjugate decays, can be described by the most general, local, derivative-free and lepton-number conserving four-fermion point interaction Hamiltonian. The point interaction permits one to use equivalent Hamiltonians which

differ in the way the fermions are grouped together [5, 19]. The older literature preferred a "charge retention" form with parity-odd and parity-even terms in which e^+ and μ^+ as the usually detected particles were grouped together [20, 15]. This had the advantage that limits to some single coupling constants could be obtained from then existing experimental results. The disadvantage was that this (charge retention) Hamiltonian represented interactions proceeding via the exchange of a neutral boson X which would carry the lepton numbers both of muon and electron and would thus not be universal. The use of a "charge changing" form, where the charged leptons are grouped with their neutrino and which is adapted to a charged boson exchange, resulted in absolute values of differences of coupling constants. Both forms mentioned above are in addition complicated by the fact that a fully parity-violating interaction like e.g. the $V-A$ interaction is represented by *four* coupling constants C_V, C'_V, C_A and C'_A.

In the following we will use a charge-changing Hamiltonian characterized by fields of definite handedness [6, 7]. The matrix element for μ decay may be denoted as [4, 21]

$$M = 4\,\frac{G_F}{\sqrt{2}} \sum_{\substack{\gamma=S,V,T \\ \varepsilon,\mu=R,L}} g^{\gamma}_{\varepsilon\mu} <\bar{e_\varepsilon}\,|\Gamma^\gamma|(\nu_e)_n><(\bar{\nu_\mu})_m|\Gamma_\gamma|\mu_\mu> \quad . \tag{2.1}$$

Here G_F is the Fermi coupling constant, while γ labels the type of interaction: Γ^S, Γ^V, Γ^T (4-scalar, 4-vector, 4-tensor). The indices ε and μ indicate the chirality (left- or right-handed) of the spinors of the charged leptons, $\varepsilon \triangleq$ electron, $\mu \triangleq$ muon. The chiralities n and m of the ν_e and the $\bar{\nu}_\mu$ spinors, respectively, are uniquely determined for given γ, ε and μ. In this picture, the coupling constants $g^{\gamma}_{\varepsilon\mu}$ have a simple physical interpretation: $n_\gamma |g^{\gamma}_{\varepsilon\mu}|^2$ is equal to the (relative) probability for a μ-handed muon to decay into an ε-handed electron by the interaction Γ^γ; the factors $n_S = 1/4$, $n_V = 1$ and $n_T = 3$ take care of the proper normalization. The standard model thus corresponds to $g^V_{LL} = 1$, all other couplings being zero.
For leptonic τ decays, μ should be substituted by τ and e by μ or e.

2.2. Observables

2.2.1. Electron Decay Distribution

In the following we give the distribution of electrons from polarized muons including the effects of the electron mass; the generalization to leptonic τ decays is obvious. We consider the decay $\mu^+ \to \bar{\nu}_\mu e^+ \nu_e$ and its charge conjugate $\mu^- \to \nu_\mu e^- \bar{\nu}_e$. In the case of double signs the upper sign refers to μ^+, the lower to μ^- decay. The kinematical range of the electron energy E_e is given by

$$m_e \leqq E_e \leqq W_{\mu e} \equiv \frac{m_\mu^2 + m_e^2}{2m_\mu} \quad . \tag{2.2}$$

With the standard reduced energy variable $x = E_e/W_{\mu e}$ this leads to

$$x_0 \leqq x \leqq 1 \tag{2.3}$$

with $x_0 = m_e/W_{\mu e}$. We note that x_0 is small for muon decay ($x_0 = 9.67 \times 10^{-3}$) and for the electronic τ decay ($x_0 = 0.29 \times 10^{-3}$), but it is not small for the muonic τ decay $x_0 = 59.2 \times 10^{-3}$).

The differential decay probability for an $e^{\pm}$ with reduced energy between x and $x + dx$, emitted at an angle between ϑ and $\vartheta + d\vartheta$ with respect to the muon's polarization $\vec{\varphi}_\mu$, and having its spin pointing into the direction of the arbitrary unit vector $\hat{\zeta}$ (see Fig. 2.1) is given by

$$\frac{d^2\Gamma}{dx\,dcos\vartheta} = \frac{1}{4} m_\mu W_{\mu e}^4 G_F^2 \sqrt{x^2 - x_0^2} (F_{IS}(x) \pm \varphi_\mu cos\vartheta \cdot F_{AS}(x)) \, (1 + \vec{\varphi}_e \cdot \hat{\zeta}) \tag{2.4}$$

where we have used $\varphi_\mu = |\vec{\varphi}_\mu|$, and where $\vec{\varphi}_e$ is the polarization vector of the $e^{\pm}$:

$$\vec{\varphi}_e = P_{T_1} \cdot \hat{x} + P_{T_2} \cdot \hat{y} + P_L \cdot \hat{z} \, . \tag{2.5}$$

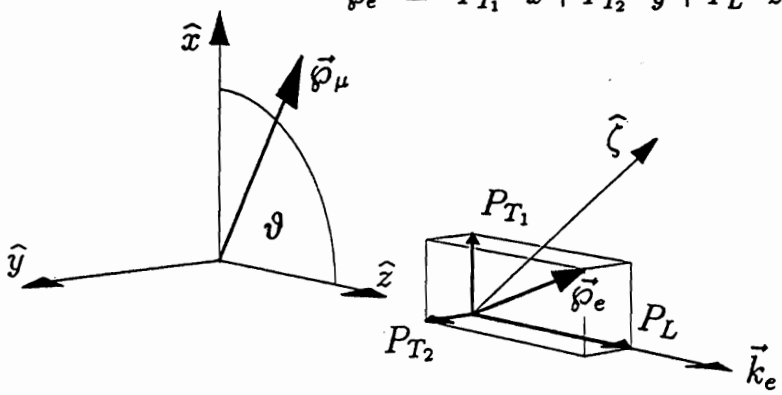

Fig. 2.1 Kinematic variables for the decay $\mu \to e\nu\bar{\nu}$ in the muon rest system.

We have defined a right-handed coordinate system with

$$\hat{z} = \frac{\vec{k}_e}{|\vec{k}_e|}, \quad \hat{y} = \frac{\vec{k}_e \times \vec{\varphi}_\mu}{|\vec{k}_e \times \vec{\varphi}_\mu|}, \quad \hat{x} = \hat{y} \times \hat{z} \quad . \tag{2.6}$$

Here $\vec{k}_e$ is the momentum vector of the electron, while P_L designates the longitudinal polarization, P_{T_1} the transverse component of $\vec{\varphi}_e$ lying in the plane defined by $\vec{k}_e$ and $\vec{\varphi}_\mu$, and P_{T_2} the component perpendicular to that plane. $P_{T_2} \neq 0$ signals violation of time reversal symmetry. These polarization components are

$$P_{T_1}(x, \vartheta) = \frac{\varphi_\mu sin\vartheta \cdot F_{T_1}(x)}{F_{IS}(x) \pm \varphi_\mu cos\vartheta \cdot F_{AS}(x)} \tag{2.7}$$

$$P_{T_2}(x, \vartheta) = \frac{\varphi_\mu sin\vartheta \cdot F_{T_2}(x)}{F_{IS}(x) \pm \varphi_\mu cos\vartheta \cdot F_{AS}(x)} \tag{2.8}$$

$$P_L(x, \vartheta) = \frac{\pm F_{IP}(x) + \varphi_\mu cos\vartheta \cdot F_{AP}(x)}{F_{IS}(x) \pm \varphi_\mu cos\vartheta \cdot F_{AS}(x)} \tag{2.9}$$

The functions $F_\nu(x)$ shall be decomposed as

$$F_\nu(x) \;=\; F_\nu^{V-A}(x) + G_\nu(x)\;, \tag{2.10}$$

where $G_\nu(x) \equiv 0$ for $g_{LL}^V = 1$ ("$V-A$"). Physics beyond the standard model would thus be contained *exclusively* in the $G_\nu(x)$. The index ν stands for IS (isotropic part of energy spectrum), AS (anisotropic part of energy spectrum), T_1 (transverse polarization P_{T_1}), T_2 (transverse polarization P_{T_2}), IP (isotropic part of longitudinal polarization) and AP (anisotropic part of longitudinal polarization). The F_ν^{V-A} do not depend on specific decay parameters:

$$F_{IS}^{V-A}(x) \;=\; \tfrac{1}{6}\{-2x^2+3x-x_0^2\} \tag{2.11}$$

$$F_{AS}^{V-A}(x) \;=\; \tfrac{1}{6}(x^2-x_0^2)^{1/2}\{2x-2+(1-x_0^2)^{1/2}\} \tag{2.12}$$

$$F_{T_1}^{V-A}(x) \;=\; -\tfrac{1}{6}(1-x)x_0 \tag{2.13}$$

$$F_{T_2}^{V-A}(x) \;=\; 0 \tag{2.14}$$

$$F_{IP}^{V-A}(x) \;=\; \tfrac{1}{6}(x^2-x_0^2)^{1/2}\{-2x+2+(1-x_0^2)^{1/2}\} \tag{2.15}$$

$$F_{AP}^{V-A}(x) \;=\; \tfrac{1}{6}\{2x^2-x-x_0^2\} \tag{2.16}$$

The functions $G_\nu(x)$ depend on the decay parameters $(\varrho, \xi'', \xi', \xi, \delta, \eta, \eta'', \alpha'/A, \beta'/A)$, where $\eta = (\alpha - 2\beta)/A$ and $\eta'' = (3\alpha + 2\beta)/A$:

$$G_{IS}(x) \;=\; \tfrac{1}{9}\left\{2(\varrho-\tfrac{3}{4})(4x^2-3x-x_0^2)+9\eta(1-x)x_0\right\} \tag{2.17}$$

$$\begin{aligned} G_{AS}(x) \;=\; & \tfrac{1}{9}(x^2-x_0^2)^{1/2}\{3(\xi-1)(1-x) \\ & +2(\xi\delta-\tfrac{3}{4})(4x-4+(1-x_0^2)^{1/2})\} \end{aligned} \tag{2.18}$$

$$\begin{aligned} G_{T_1}(x) \;=\; & \tfrac{1}{12}\left\{-2[(\xi''-1)+12(\varrho-\tfrac{3}{4})](1-x)x_0-3\eta(x^2-x_0^2)\right. \\ & \left.+\eta''(-3x^2+4x-x_0^2)\right\} \end{aligned} \tag{2.19}$$

$$G_{T_2}(x) \;=\; \tfrac{1}{3}(x^2-x_0^2)^{1/2}\{3\frac{\alpha'}{A}(1-x)+2\frac{\beta'}{A}(1-x_0^2)^{1/2}\} \tag{2.20}$$

$$\begin{aligned} G_{IP}(x) \;=\; & \tfrac{1}{54}(x^2-x_0^2)^{1/2}\{(\xi'-1)(-2x+2+(1-x_0^2)^{1/2}) \\ & +4\xi(\delta-\tfrac{3}{4})(4x-4+(1-x_0^2)^{1/2})\} \end{aligned} \tag{2.21}$$

$$G_{AP}(x) = \frac{1}{6}\{(\xi'' - 1)(2x^2 - x - x_0^2) + 4(\varrho - \frac{3}{4})(4x^2 - 3x - x_0^2) + 2\eta''(1-x)x_0\} \quad (2.22)$$

Table 2.1 gives an overview on the influence of the decay parameters to the various observables.

Table 2.1 Dependence of the functions G_ν on the various decay parameters. The G_ν describe the effects of non-$V-A$ contributions to the observables of the electron. Full dependence of a G_ν to a decay parameter is expressed by an "x", restricted dependence by an "(x)". Restricted dependence means proportionality to $x_0 = m_e/W_{\mu e} \approx 10^{-2}$.

Observable	ν	ϱ	ξ''	ξ'	ξ	δ	η	η''	α'/A	β'/A
Isotropic part spectrum	IS	x					(x)			
Anisotropic part of spectrum	AS				x	x				
Transverse electron polarization P_{T_1}	T_1	(x)	(x)				x	x		
Transverse electron polarization P_{T_2} (T-violating)	T_2								x	x
Isotropic part of longitudinal polarization P_L	IP			x	x	x				
Anisotropic part of longitudinal polarization P_L	AP	x	x					(x)		

2.2.2. Electron Neutrino Energy Distribution

It has recently been realized that present experiments which detect the ν_e from the decay of unpolarized μ^+ by the reaction $^{12}C(\nu_e, e^-)^{12}N(g.s.)$ not only determine the neutrino absorption cross section but also measure the ν_e energy spectrum [22]. The energy spectrum can be described by spectrum shape parameters ω_L and η_L for left-handed and ω_R and η_R for right-handed ν_e. In contrast to the energy spectrum of the electrons it allows a new null-test of the standard model [22] (see Sect. 2.4.6). The right-handed ν_e cannot be detected as they are sterile in matter. For the energy spectrum of the left-handed ν_e one obtains [23]

$$\frac{d\Gamma_L}{dy} = \frac{m_\mu^5 G_F^2}{16\pi^3} \cdot Q_L^{\nu_e} \cdot \{F_1(y) + \omega_L \cdot F_2(y) + \eta_L x_0 F_3(y)\} \quad (2.23)$$

Here $d\Gamma_L/dy$ is the probability of a left-handed ν_e to be emitted with the reduced energy $y = 2E_\nu/m_\mu$. The probability $Q_L^{\nu_e}$ of the ν_e to be left-handed, the spectral shape parameter ω_L and the low energy parameter η_L are [23]

$$\begin{aligned} Q_L^{\nu_e} &= \tfrac{1}{4}|g_{RL}^S|^2 + \tfrac{1}{4}|g_{RR}^S|^2 + |g_{LL}^V|^2 + |g_{LR}^V|^2 + 3|g_{RL}^T|^2 \\ &= \tfrac{1}{2}(1 + \wp_{\nu_e}) \end{aligned} \tag{2.24}$$

$$\omega_L = \frac{3}{4}\frac{\left\{|g_{RR}^S|^2 + 4|g_{LR}^V|^2 + |g_{RL}^S + 2g_{RL}^T|^2\right\}}{\{|g_{RL}^S|^2 + |g_{RR}^S|^2 + 4|g_{LL}^V|^2 + 4|g_{LR}^V|^2 + 12|g_{RL}^T|^2\}} \tag{2.25}$$

$$\eta_L = 2\frac{Re\left\{g_{LL}^V g_{RR}^{S*} + g_{LR}^V(g_{RL}^{S*} + 6g_{RL}^{T*})\right\}}{\{|g_{RL}^S|^2 + |g_{RR}^S|^2 + 4|g_{LL}^V|^2 + 4|g_{LR}^V|^2 + 12|g_{RL}^T|^2\}}, \tag{2.26}$$

where $\wp_{\nu_e}$ denotes the longitudinal polarization of the ν_e. The functions $F_1(y)$, $F_2(y)$ and $F_3(y)$ are given by

$$F_1(y) = \frac{(1 - x_0^2 - y)^2 y^2}{1 - y} \tag{2.27}$$

$$F_2(y) = \tfrac{2}{9}\frac{(1 - x_0^2 - y)^2 y^2}{(1 - y)^3}(-4y^2 + y(7 - x_0^2) - 3 + 3x_0^2) \tag{2.28}$$

$$F_3(y) = \frac{(1 - x_0^2 - y)^2 y^2}{(1 - y)^2} \tag{2.29}$$

The corresponding quantities $d\Gamma_R/dy$, $Q_R^{\nu_e}$, ω_R and η_R for the energy spectrum of the right-handed ν_e may be obtained from Eqs. 2.23-2.26 simply by the substitutions $R \Leftrightarrow L$ for every chirality index and by $\wp_{\nu_e} \rightarrow -\wp_{\bar{\nu}_e}$. The size of ω_k and η_k $(k = R, L)$ is constrained by the fact that $g_{LL}^V \approx 1$, and $g_{e\mu}^\gamma \approx 0$ for all other interactions. One therefore finds $\omega_L \gtrapprox 0$ and $\eta_L \approx 0$, but $0 \leqq \omega_R \leqq 1$ and $-1 \leqq \eta_R \leqq 1$. The term with $\eta_L x_0 F_3(y)$ can be neglected because both η_L and the factor $x_0 \approx 10^{-2}$ are small. Thus the energy spectrum of left-handed ν_e which *can be* detected by absorption on ^{12}C is described effectively by *two* observables, namely $Q_L^{\nu_e} = 1 - Q_R^{\nu_e}$ which is a measure of the total rate and therefore of the ν_e polarization, and ω_L which describes the shape of the spectrum. The probability $Q_L^{\nu_e}$ can be determined from the total absorption rate, if the absolute absorption cross section σ_A is known with sufficient precision.

2.2.3. Inverse Muon Decay

The reaction $\nu_\mu e^- \rightarrow \mu^- \nu_e$, usually called *inverse muon decay*, shall be governed by the same Hamiltonian as (normal) muon decay. Its measurement will, in contrast to normal muon decay, allow to separate g_{LL}^S from g_{LL}^V and thus to

complete the experimental proof of $V-A$.

The normalized total cross section S is obtained by integrating over the electron energy and the energy spectrum of the incoming ν_μ and by dividing by the theoretical value for a pure $V-A$ interaction [24]. S has been calculated for the general decay interaction [25, 7]. In terms of our coupling constants it is given by [26]

$$S = \tfrac{1}{2}(1+\wp_{\nu_\mu})\cdot S_R + \tfrac{1}{2}(1-\wp_{\nu_\mu})\cdot S_L, \tag{2.30}$$

where $\wp_{\nu_\mu}$ is the longitudinal polarization of the incoming ν_μ. The quantities S_R and S_L are the normalized cross sections for right- respectively left-handed ν_μ:

$$S_R = \tfrac{3}{32}|g^S_{LL}|^2 + |g^V_{RR}|^2 + \tfrac{3}{8}|g^V_{LR}|^2 + \tfrac{3}{32}|g^S_{RL} - \tfrac{10}{3}g^T_{RL}|^2 + \tfrac{4}{3}|g^T_{RL}|^2 \tag{2.31}$$

$$S_L = \tfrac{3}{32}|g^S_{RR}|^2 + |g^V_{LL}|^2 + \tfrac{3}{8}|g^V_{RL}|^2 + \tfrac{3}{32}|g^S_{LR} - \tfrac{10}{3}g^T_{LR}|^2 + \tfrac{4}{3}|g^T_{LR}|^2 \tag{2.32}$$

We will see that the longitudinal polarization $\wp_{\nu_\mu}$ of the ν_μ from π^+ decay is close to -1 within 3.2×10^{-3} [27, 28] so that the couplings in S_R cannot contribute to S. We will further see that normal muon decay places stringent limits on all the couplings in S_L except on g^V_{LL}. Therefore S just measures $|g^V_{LL}|^2$. This has made it possible to derive a lower limit for $|g^V_{LL}|$ for the first time and thus to establish $V-A$ as the dominant interaction in muon decay [4].

2.2.4. Radiative Muon Decays

Radiative muon decay, $\mu^+ \to \bar{\nu}_\mu e^+ \nu_e \gamma$, is treated in detail in Ref. [29]. The electron and gamma spectra depend on the decay parameters ϱ and δ as well as on the two new combinations $\bar{\eta}$ and $\xi\cdot\kappa$ [30]:

$$\bar{\eta} = \tfrac{1}{A}(a+2c) = \tfrac{1}{4}(7-12\varrho-\xi'') \tag{2.33}$$

$$\xi\cdot\kappa = \tfrac{1}{A}(a'+2c') = -\tfrac{1}{12}(3\xi+3\xi'-8\xi\delta) \tag{2.34}$$

The parameter $\bar{\eta}$, in particular, is positive semidefinite and zero in the standard model. It can be expressed by a sum of absolute squares of combinations of coupling constants:

$$\begin{aligned}\bar{\eta} = {} & (|g^V_{RL}|^2 + |g^V_{LR}|^2) + \tfrac{1}{8}(|g^S_{LR}+2g^T_{LR}|^2 + |g^S_{RL}+2g^T_{RL}|^2) \\ & +2(|g^T_{LR}|^2 + |g^T_{RL}|^2)\,.\end{aligned} \tag{2.35}$$

This allows one to get upper limits for each term separately.

It is also worthwhile to mention the decay $\mu^+ \to \bar{\nu}_\mu e^+ \nu_e e^+ e^-$ which has been calculated recently in terms of the most general decay interaction (Eq. 2.1) [31]. The decay distribution depends on the probabilities $Q_{e\mu}$ and on the bilinear quantities $B_{RL} = (a+a')/(2A)$, $B_{LR} = (a-a')/(2A)$ defined in Ref. [4].

2.3. Lorentz Structure

2.3.1. Decay Parameters

The nine parameters (ϱ, ξ'', ξ', ξ, δ, η, η'', α'/A, β'/A) describing the *electron's spectrum, decay asymmetry* and *polarization vector* can be represented [20] by the intermediate quantities (a, a', α, α', b, b', β, β', c, c'), whose values are known from experiment [32]. They are all real, bilinear combinations of the coupling constants:

$$a = 16(|g^V_{RL}|^2 + |g^V_{LR}|^2) + |g^S_{RL} + 6g^T_{RL}|^2 + |g^S_{LR} + 6g^T_{LR}|^2 \quad (2.36)$$

$$a' = 16(|g^V_{RL}|^2 - |g^V_{LR}|^2) + |g^S_{RL} + 6g^T_{RL}|^2 - |g^S_{LR} + 6g^T_{LR}|^2 \quad (2.37)$$

$$\alpha = 8Re\left\{g^V_{RL}(g^{S*}_{LR} + 6g^{T*}_{LR}) + g^V_{LR}(g^{S*}_{RL} + 6g^{T*}_{RL})\right\} \quad (2.38)$$

$$\alpha' = 8Im\left\{g^V_{LR}(g^{S*}_{RL} + 6g^{T*}_{RL}) - g^V_{RL}(g^{S*}_{LR} + 6g^{T*}_{LR})\right\} \quad (2.39)$$

$$b = 4(|g^V_{RR}|^2 + |g^V_{LL}|^2) + |g^S_{RR}|^2 + |g^S_{LL}|^2 \quad (2.40)$$

$$b' = 4(|g^V_{RR}|^2 - |g^V_{LL}|^2) + |g^S_{RR}|^2 - |g^S_{LL}|^2 \quad (2.41)$$

$$\beta = -4Re\left\{g^V_{RR}g^{S*}_{LL} + g^V_{LL}g^{S*}_{RR}\right\} \quad (2.42)$$

$$\beta' = 4Im\left\{g^V_{RR}g^{S*}_{LL} - g^V_{LL}g^{S*}_{RR}\right\} \quad (2.43)$$

$$c = \tfrac{1}{2}\left\{|g^S_{RL} - 2g^T_{RL}|^2 + |g^S_{LR} - 2g^T_{LR}|^2\right\} \quad (2.44)$$

$$c' = \tfrac{1}{2}\left\{|g^S_{RL} - 2g^T_{RL}|^2 - |g^S_{LR} - 2g^T_{LR}|^2\right\} \quad (2.45)$$

From Eqs. 2.36-2.45 it can be seen that these quantities are not completely independent. The transformation from the 20-dimensional space of the $g^\gamma_{\epsilon\mu}$ to the 10-dimensional space of the $\{a, ..., c'\}$ leads to the following six constraints [32]:

$$a \geqq 0 \quad (2.46) \qquad a^2 \geqq a'^2 + \alpha^2 + \alpha'^2 \quad (2.49)$$

$$b \geqq 0 \quad (2.47) \qquad b^2 \geqq b'^2 + \beta^2 + \beta'^2 \quad (2.50)$$

$$c \geqq 0 \quad (2.48) \qquad c^2 \geqq c'^2 \quad (2.51)$$

These constraints are very important for any general analysis of muon decay, since they strongly influence the final errors of the quantities they relate.

Table 2.2 Allowed ranges, V-A values and experimental results (in units of 10^{-3}) for the muon decay parameters. Upper and lower limits are given with 90% *c.l.*

Decay parameter	Minimum	Maximum	$V-A$ value	Experimental result $[10^{-3}]$	Ref.	Comments
ϱ	0	1	3/4	751.8 ± 2.6	[33]	
ξ''	-7/3	3	1	650 ± 360	[34]	
ξ	-3	3	1	1004.5 ± 8.6	[35, 36]	
$\wp_\mu^\pi \xi$	-3	3	1	1002.7 ± 8.4	[35]	$\pi^+ \to \mu^+ \nu_\mu$
$\wp_\mu^K \xi$	-3	3	1	1001.3 ± 6.1	[37]	$K^+ \to \mu^+ \nu_\mu$
$\xi\delta$	-1	1	3/4			
δ	$-\infty$	∞	3/4	748.6 ± 3.8	[28]	
ξ'	-1	1	1	998 ± 45	[34]	
$\xi\delta/\varrho$	-1	1	1	> 996.8	[36]	$\wp_\mu \xi\delta/\varrho$
η	-1	1	0	-7 ± 13	[32]	
η''	-3	3	0	12 ± 16	[32]	
α'/A	-1	1	0	-0.2 ± 4.3	[32]	
β'/A	-1/4	1/4	0	1.5 ± 6.3	[32]	
ω_L	0	1	0		[23, 38]	$^{12}C(\nu_e, e^-)^{12}N$
S_L	0	1	1	1006 ± 47	[39, 40]	$\nu_\mu e^- \to \mu^- \nu_e$
$\bar{\eta}$	0	1	0	-30 ± 100	[29]	$\mu^+ \to \bar{\nu}_\mu e^+ \nu_e \gamma$
Q_{RR}	0	1	0	< 2.0	[4]	
Q_{LR}	0	1	0	< 3.9	[4]	
Q_{RL}	0	1	0	< 45.0	[4]	
Q_{LL}	0	1	1	> 949.0	[4]	
Q_R^μ	0	1	0	< 7.7		
Q_R^e	0	1	0	< 38.0		
$Q_R^{\nu_\mu}$	0	1	0	< 80.0		
$Q_R^{\nu_e}$	0	1	0	< 80.0	[23]	

The decay parameters are given by

$$\varrho = \tfrac{1}{A}(3b + 6c) \quad (2.52)$$

$$\xi'' = \tfrac{1}{A}(3a + 4b - 14c) \quad (2.53)$$

$$\xi = -\tfrac{1}{A}(3a' + 4b' - 14c') \quad (2.54)$$

$$\xi\delta = \tfrac{1}{A}(-3b' + 6c') \quad (2.55)$$

$$\xi' = -\tfrac{1}{A}(a' + 4b' + 6c') \quad (2.56)$$

$$\eta = \tfrac{1}{A}(\alpha - 2\beta) \quad (2.57)$$

$$\eta'' = \tfrac{1}{A}(3\alpha + 2\beta) \quad (2.58)$$

The parameters α'/A and β'/A are determined directly. The allowed range, the

$V - A$ predictions and the experimental results of the muon decay parameters, which are not all independent, are given in Table 2.2.

2.3.2. Complete Determination of the Lorentz Structure

The precise measurement of individual decay parameters alone generally does not give conclusive information about the decay interaction due to the many different couplings and the interference terms between them. An example is the famous Michael parameter ϱ. A precise measurement yielding the V-A value of 3/4 by no means establishes the V-A interaction. In fact any interaction consisting of an arbitrary combination of g^S_{LL}, g^S_{LR}, g^S_{RL}, g^S_{RR}, g^V_{RR} and g^V_{LL} will yield exactly $\varrho = \frac{3}{4}$ [41]. This can be seen if we write ϱ in the form [42]

$$\varrho - \tfrac{3}{4} = -\tfrac{3}{4}\left\{|g^V_{LR}|^2 + |g^V_{RL}|^2 + 2(|g^T_{LR}|^2 + |g^T_{RL}|^2) + Re(g^S_{LR}g^{T*}_{LR} + g^S_{RL}g^{T*}_{RL})\right\} . \tag{2.59}$$

For $\varrho = \frac{3}{4}$ and $g^T_{LR} = g^T_{RL} = 0$ (no tensor interaction) we find $g^V_{LR} = g^V_{RL} = 0$, with all the remaining six couplings being arbitrary !

The magnitude of the decay interaction is contained in the Fermi coupling constant G_F. Thus the $g^\gamma_{\epsilon\mu}$ may be normalized, dimensionless coupling constants, resulting in

$$A \equiv a + 4b + 6c = 16 \tag{2.60}$$

or equivalently,

$$\begin{aligned} &\tfrac{1}{4}|g^S_{RR}|^2 + \tfrac{1}{4}|g^S_{RL}|^2 + \tfrac{1}{4}|g^S_{LR}|^2 + \tfrac{1}{4}|g^S_{LL}|^2 \\ + \;&|g^V_{RR}|^2 + |g^V_{RL}|^2 + |g^V_{LR}|^2 + |g^V_{LL}|^2 \\ &+ 3|g^T_{RL}|^2 + 3|g^T_{LR}|^2 = 1 \end{aligned} \tag{2.61}$$

By rearranging the terms in Eq. 2.61 according to the chiralities ϵ and μ of the electron and the muon (ϵ, $\mu = R, L$) it is possible to define the four quantities $Q_{\epsilon\mu}$:

$$Q_{RR} = \tfrac{1}{4}|g^S_{RR}|^2 + |g^V_{RR}|^2 \tag{2.62}$$

$$Q_{LR} = \tfrac{1}{4}|g^S_{LR}|^2 + |g^V_{LR}|^2 + 3|g^T_{LR}|^2 \tag{2.63}$$

$$Q_{RL} = \tfrac{1}{4}|g^S_{RL}|^2 + |g^V_{RL}|^2 + 3|g^T_{RL}|^2 \tag{2.64}$$

$$Q_{LL} = \tfrac{1}{4}|g^S_{LL}|^2 + |g^V_{LL}|^2 \tag{2.65}$$

We note that $0 \leq Q_{\epsilon\mu} \leq 1$ and $\sum_{\epsilon,\mu} Q_{\epsilon\mu} = 1$. $Q_{\epsilon\mu}$ is then the probability for the decay of a muon of handedness μ into an electron of handedness ϵ. The main point is now that the $Q_{\epsilon\mu}$ can be expressed by the known quantities $\{a, ..., c'\}$ [4]:

$$Q_{RR} = 2(b+b')/A \tag{2.66}$$

$$Q_{LR} = [(a-a')+6(c-c')]/(2A) \tag{2.67}$$

$$Q_{RL} = [(a+a')+6(c+c')]/(2A) \tag{2.68}$$

$$Q_{LL} = 2(b-b')/A \tag{2.69}$$

The existing measurements show that the three quantities Q_{RR}, Q_{LR} and Q_{RL} are zero, within errors. This gives upper limits to the absolute values of eight of the ten complex coupling constants $g^{\gamma}_{\epsilon\mu}$. Furthermore we find that Q_{LL} is bounded by a lower limit which confirms that both muon and electron are left-handed. It can be seen from Eq. 2.65, however, that the data from the measurements of the μ and the e do not allow one to distinguish vector (g^{V}_{LL}) from scalar (g^{S}_{LL}) interaction. This type of ambiguity has been noted before in the context of a different Hamiltonian [8], and electron - neutrino correlation measurements (not performed up to date) have been proposed. It has been shown that one can resolve this ambiguity also with the information from inverse muon decay [4]. The total rate S, normalized to the rate predicted by $V-A$, for the reaction $\nu_\mu + e^- \rightarrow \mu^- + \nu_e$ with ν_μ of negative helicity has been found to be close to 1 [39, 40]. S depends effectively only on those five coupling constants g^{V}_{LL}, g^{V}_{RL}, g^{S}_{LR}, g^{T}_{LR} and g^{S}_{RR} which describe interactions with left-handed ν_μ. The four latter ones are found to be small. One thus obtains [4]

$$S = |g^{V}_{LL}|^2 \tag{2.70}$$

which yields a *lower* limit for $|g^{V}_{LL}|$, and through the normalization requirement Eq. 2.61 an *upper* limit for the remaining $|g^{S}_{LL}|$:

$$|g^{S}_{LL}| < 2\sqrt{1-S} \tag{2.71}$$

Thus the weak interaction has been completely determined for muon decay using only data from this purely leptonic interaction. The results are shown in Fig. 2.2 where each of the ten complex normalized coupling constants $g^{\prime\gamma}_{\epsilon\mu} = g^{\gamma}_{\epsilon\mu}/\max(|g^{\gamma}_{\epsilon\mu}|)$ is given within one of the squares defined uniquely by the handednesses of the electron and the muon and by the type of interaction. The outer circles display the mathematical limits for the $g^{\prime\gamma}_{\epsilon\mu}$ in the complex plane, while the inner circles for nine of the $g^{\prime\gamma}_{\epsilon\mu}$ show the areas still allowed by experiments (90% *c.l.*). For $g^{\prime V}_{LL}$, which has been chosen to be real, one gets the small line close to $g^{\prime V}_{LL} = 1$ in agreement with the standard model.

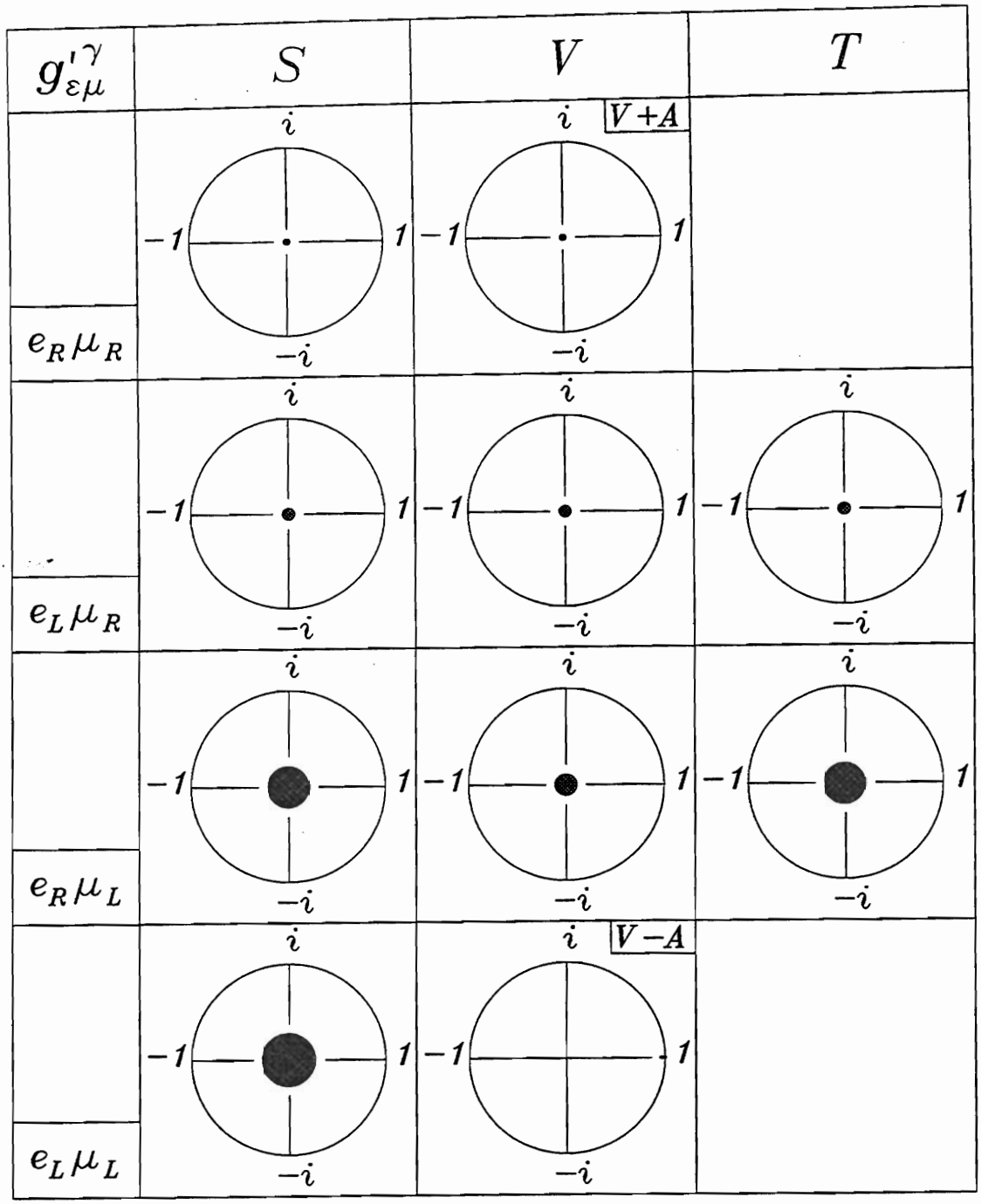

Fig. 2.2 90% *c.l.* limits for the reduced coupling constants $g^{\gamma}_{\varepsilon\mu} = g^{\gamma}_{\varepsilon\mu}/\max(|g^{\gamma}_{\varepsilon\mu}|)$ describing the decay $\mu^+ \to \bar{\nu}_\mu e^+ \nu_e$ (From Ref. [26]. Updated limits from [28, 40]). Each coupling is uniquely determined by the handednesses ε and μ of the electron and the muon, respectively, and by the type of interaction $\gamma = S$, V or T. The maximal possible values of the coupling constants are 2, 1 and $1/\sqrt{3}$ for $\gamma = S$, V resp. T.

2.3.3. *Minimal Set of Measurements*

It has been shown in the previous section that a limited amount of measurements allows one to completely determine the Lorentz structure of the interaction. This has been possible because the quantities $Q_{e\mu}$ are positive semidefinite forms of the coupling constants $g^{\gamma}_{\varepsilon\mu}$, and because they can be expressed by experimental results. By summing over the first or over the second index one obtains the probabilities Q^{μ}_{R} and Q^{e}_{R} for the muon and for the electron, respectively, to be right-handed [26]:

$$\begin{aligned} Q^{\mu}_{R} &= \tfrac{1}{4}|g^{S}_{RR}|^2 + \tfrac{1}{4}|g^{S}_{LR}|^2 + |g^{V}_{RR}|^2 + |g^{V}_{LR}|^2 + 3|g^{T}_{LR}|^2 \\ &= \tfrac{1}{2}\left\{1 + \tfrac{1}{9}(3\xi - 16\xi\delta)\right\} \qquad (2.72) \\ Q^{e}_{R} &= \tfrac{1}{4}|g^{S}_{RR}|^2 + \tfrac{1}{4}|g^{S}_{RL}|^2 + |g^{V}_{RR}|^2 + |g^{V}_{RL}|^2 + 3|g^{T}_{RL}|^2 \\ &= \tfrac{1}{2}(1 - \xi') \qquad (2.73) \end{aligned}$$

Thus Q^{μ}_{R} depends on the two asymmetry parameters ξ and δ which contain the information of how much right-handed the muon can be, while Q^{e}_{R} depends exclusively on the average electron polarization ξ'.

One can also derive the probabilities $Q^{\bar{\nu}_e}_{R}$ and $Q^{\nu_\mu}_{R}$ for the $\bar{\nu}_e$ and ν_μ to be right-handed [23]. In this connection we note that we strictly keep apart the concepts of *chirality* as a transformation property of the fermion spinors and of *helicity* as the spin projection of a pure particle state onto the direction of motion. Thus for $V-A$ ($g^{V}_{LL}=1$) both $\bar{\nu}_\mu$ and ν_e are left-handed, but of opposite helicity. The quantities $Q^{\bar{\nu}_e}_{R}$ and $Q^{\nu_\mu}_{R}$ can be obtained by remembering that scalar and tensor interactions change the chirality of a fermion at the vertex while vector interactions conserve it:

$$\begin{aligned} Q^{\bar{\nu}_e}_{R} &= \tfrac{1}{4}|g^{S}_{LL}|^2 + \tfrac{1}{4}|g^{S}_{LR}|^2 + |g^{V}_{RR}|^2 + |g^{V}_{RL}|^2 + 3|g^{T}_{LR}|^2 \\ &= \tfrac{1}{2}(1 - \wp_{\bar{\nu}_e}) \qquad (2.74) \\ Q^{\nu_\mu}_{R} &= \tfrac{1}{4}|g^{S}_{LL}|^2 + \tfrac{1}{4}|g^{S}_{RL}|^2 + |g^{V}_{RR}|^2 + |g^{V}_{LR}|^2 + 3|g^{T}_{RL}|^2 \\ &= \tfrac{1}{2}(1 + \wp_{\nu_\mu}) \ , \qquad (2.75) \end{aligned}$$

where $\wp_{\bar{\nu}_e}$ and $\wp_{\nu_\mu}$ denote the longitudinal polarizations of the neutrinos. To determine the interaction it is sufficient that three of the Q^{α}_{R} are measured and found to be zero, within errors. This amounts to measuring the polarization of at least one of the neutrinos precisely, as has been proposed for $\wp_{\nu_e}$ which can be deduced from a measurement of the total rate of absorption of the ν_e on ^{12}C (see Sect. 2.2.2). An alternative to *measuring* the polarization of the neutrinos from μ decay is to induce inverse muon decay with ν_μ from π^+ decay [39, 40] whose polarization is *precisely known* [27] (see Sect. 2.3.2). We conclude that only five of

nineteen possible measurements are necessary to completely determine the $(V-A)$ interaction:

(1) Muon lifetime which yields the magnitude

(2,3) Asymmetry parameters ξ and δ which yield the muon chirality

(4) Electron longitudinal polarization which yields the electron chirality, and

(5) Inverse muon decay with ν_μ of known helicity or rate of absorption of ν_e from muon decay.

2.4. Measurements

2.4.1. Lifetime

The total rate Γ of muon decay exhibits the strength G_F which is generally assumed to be universal for the charged weak interaction:

$$\Gamma = \frac{G_F^2 m_\mu^5}{192\pi^3} \cdot \{1 + 4\eta\frac{m_e}{m_\mu} - 8(\frac{m_e}{m_\mu})^2\} \cdot f_W \cdot f_r, \tag{2.76}$$

where $f_W = 1 + \frac{3}{5}(m_\mu/m_W)^2$, $f_r = 1 - \frac{\alpha}{2\pi}(\pi^2 - \frac{25}{4})$ and $m_e/m_\mu = 4.84 \times 10^{-3}$. The factor f_W represents the influence of the finite mass m_W of the intermediate boson. The smallness of this term for muon (and for leptonic tau) decay justifies the analysis based on the four-fermion point interaction of Eq. 2.1. The radiative corrections are finite for the vector type interaction $\gamma = V$ (See Ref. [15],[43]-[51]). To first order, $f_r = 0.996$, independent of the lepton masses. The parameter η influences the rate [52], the spectrum and the polarization of the electron. The *uncertainty in* G_F derived from lepton decay is *dominated by the uncertainty in* η. This fact *is most often ignored*, for muon as well as for tau decay. (See also Sects. 2.4.2. and 3.2.)

Experimental difficulties in the measurement of the muon lifetime arise from the different fluctuations of the physical processes which detect the moment of the birth of the muon and of the occurrence of the decay electron. Special care is needed because muon spin rotation and the range of electron energies (see e.g. [53]) tend to distort the time spectrum. The average muon mean life is

$$\tau_\mu = (2\,197.03 \pm 0.04)\ ns$$

which corresponds to

$$G_F = (11\,664.1 \pm 0.2) \times 10^{-9}(\hbar c)^3 GeV^{-2},$$

where $\eta = 0$ has been assumed. The present uncertainty due to the term $4\eta m_e/m_\mu$ is 20 *times larger.* As seen from

$$\eta = \tfrac{1}{2} Re \left\{ g_{LL}^{V} g_{RR}^{S*} + g_{RR}^{V} g_{LL}^{S*} + g_{LR}^{V} (g_{RL}^{S*} + 6 g_{RL}^{T*}) + g_{RL}^{V} (g_{LR}^{S*} + 6 g_{LR}^{T*}) \right\} \quad (2.77)$$

a right-handed scalar interaction ($Re\ g_{RR}^{S} \neq 0$) would cause $\eta \neq 0$ in first order.

2.4.2. Electron Energy Spectrum

The continuous electron energy spectrum shows that the muon decays into three light particles (at least). The electrons with high energies are most probable. This reflects the fact that the two unobserved neutral particles are emitted preferentially in the same direction, and suggests that they are not identical fermions [52]. The existence of the reaction ("inverse muon decay" [24, 39, 40])

$$\nu_\mu e^- \rightarrow \mu^- + neutral$$

and of the chain [54]

$$\begin{aligned} \mu^+ &\rightarrow e^+ + neutral(1) + neutral(2) \\ neutral(1) + n &\rightarrow e^- + X \end{aligned}$$

confirms that $neutral(1)$ is ν_e and $neutral(2)$ is $\bar{\nu}_\mu$. The identity of the neutrinos in muon decay with those in pion or in nuclear beta decay has been studied in Refs. [12, 55].

The electron energy spectrum derived from Eq. 2.1 for the decay of unpolarized muons ($\wp_\mu = 0$) recorded by a spectrometer insensitive to electron polarization ($< \hat{\zeta} >= 0$) is given by Eq. 2.4:

$$\frac{d\Gamma}{dx} \sim \sqrt{x^2 - x_0^2} \left\{ (-x^2 + x) + \tfrac{2}{9} \varrho (4x^2 - 3x - x_0^2) + \eta (1 - x) x_0 \right\} \quad (2.78)$$

Radiative corrections are sizeable and have in addition to be included (See Ref. [15],[43]-[51]). ϱ is of influence at the upper end, η at the lower end of the spectrum. Precise experimental determinations of η from the spectrum shape have been difficult because the sensitivity to η is diminished by a factor of $x_0 \approx 10^{-2}$ and because it is not entirely possible to suppress all unwanted bremsstrahlung processes in the detector material which tend to populate the low energy region in a way that cannot be precisely predicted.

η has also been determined from the energy dependence of the transverse polarization P_{T_1} (see Eq. 2.19 and Sect. 2.4.5), where it occurs *without* the suppression factor x_0. The results are

$$\begin{aligned} \eta &= (-120 \pm 210) \times 10^{-3} \quad \text{[33] from spectrum measurement} \\ &= (\ -11 \pm\ 85) \times 10^{-3} \quad \text{[32] from } P_{T_1} \\ &= (\ \ -7 \pm\ 13) \times 10^{-3} \quad \text{[32] from global fit to all measurements} \end{aligned}$$

in agreement with $\eta = 0$.

The knowledge of η is important for a precise determination not only of the Fermi coupling constant but also of ϱ. Given a measured spectrum with data in a limited energy range (such as Fig. 2.3 [56]), the statistical accuracy depends strongly on any prior knowledge of η, as pointed out by Ref. [57] and as further

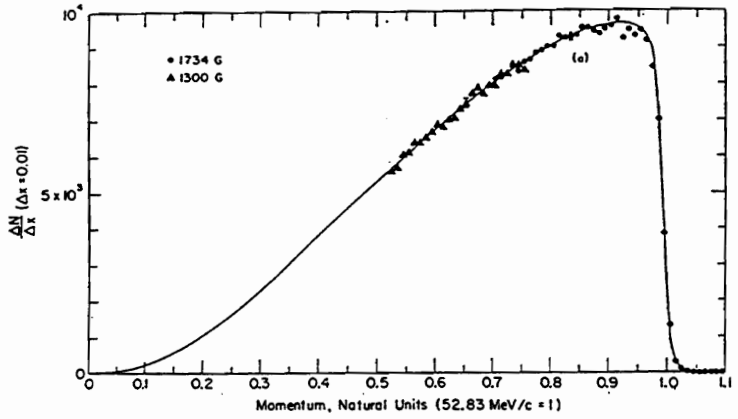

Fig. 2.3 Positron energy spectrum of μ^+ decay [56]. Solid line: Eq. 2.76 with $\varrho = 0.760$, $\eta = 0$, and radiative corrections included.

discussed in Ref. [56]. The experimental difficulties include the precise knowledge of the resolution function of the spectrometer, i.e. the calibration over a wide range of energies. Thin-walled acoustical [58, 59] or wire spark chambers [56] have been used to ensure that the positrons follow well defined trajectories through a homogeneous magnetic field. The present average value

$$\varrho = (751.8 \pm 2.6) \times 10^{-3}$$

agrees with $\varrho = 3/4$. It is mainly given by an experiment of 1966 [59]. For the determination of the muon decay interaction, ϱ is of secondary importance, as discussed in Sect. 2.3.2. It is, however, sensitive to $W_R - W_L$ mixing in left-right symmetric models and to supersymmetric muon decays (see Fig. 2.10 and Table 2.3)

2.4.3. Electron Decay Asymmetry

The measurement of the electron decay asymmetry $\mathcal{A}(x)$ from polarized muons determines how strong the chiral components (L, R) of the muon take part in the interaction. It has been used to search for right-handed currents and other muon decay modes outside the standard model.

If the combination

$$\begin{aligned} \tfrac{1}{2}(1 + \tfrac{1}{3}\xi - \tfrac{16}{9} \cdot \xi \cdot \delta) &= \tfrac{1}{4}|g^S_{RR}|^2 + \tfrac{1}{4}|g^S_{LR}|^2 + |g^V_{RR}|^2 + |g^V_{LR}|^2 + 3|g^T_{LR}|^2 \\ &\equiv Q_{RR} + Q_{LR} \equiv Q^\mu_R \end{aligned} \tag{2.79}$$

would take a value different from zero, then a coupling to the right-handed component of the muon would have to exist, i.e. at least one $g^\gamma_{\epsilon R} \neq 0$. Conversely, the

finding that $Q_R^\mu = 0$ proves that the coupling acts exclusively on the left-handed component of the muon.

The distribution of the directions of flight of the positrons (electrons) is given by Eq. 2.4

$$\frac{d^2\Gamma}{dx\,d\cos\vartheta}(x,\vartheta) \equiv \mathrm{w}(x,\vartheta) \sim \ (F_{IS}(x) \ \pm \ \wp_\mu \cdot cos\vartheta \cdot F_{AS}(x)) \quad . \tag{2.80}$$

It depends on the reduced energy x, the angle ϑ between the muon polarization and the positron momentum, as chosen by the detector, and on the amount of polarization $\wp_\mu \geq 0$. The asymmetry

$$\mathcal{A}(x) \equiv \frac{\mathrm{w}(x,o) - \mathrm{w}(x,\pi)}{\mathrm{w}(x,o) + \mathrm{w}(x,\pi)} = \wp_\mu \cdot \frac{F_{AS}(x)}{F_{IS}(x)} \tag{2.81}$$

depends on the parameters ϱ, η, ξ and $\xi\delta$ (see Eqs. 2.10-2.12, 2.17 and 2.18).

We discuss now the experimental situations in which the parameters δ and ξ have their special influence. The energy x_δ where the asymmetry vanishes, $\mathcal{A}(x_\delta) = 0$, depends on the parameter δ only. Solving x_δ for δ, we obtain

$$(\delta - \frac{3}{4}) \ \approx \ \frac{3}{4} \cdot \frac{1 - 2x_\delta - (\sqrt{1 - x_0^2} - 1)}{4x_\delta - 3 + \sqrt{1 - x_0^2} - 1} \tag{2.82}$$

This allows one to determine δ from an asymmetry measurement as a function of the energy using polarized muons ($\wp_\mu \neq 0$). The knowledge of the magnitude $\wp_\mu$ of their polarization is not required.

The distributions of the directions of flight of the positrons (electrons) as seen by an apparatus which is equally sensitive to positrons of all energies is given by

$$\begin{aligned} \frac{d\Gamma}{d\cos\vartheta}(\vartheta) \ &\sim \ \int_{x_0}^{1} dx \cdot \sqrt{x^2 - x_0^2} \cdot F_{IS}(x) \pm \wp_\mu \cdot cos\vartheta \cdot \int_{x_0}^{1} dx \cdot \sqrt{x^2 - x_0^2} \cdot F_{AS}(x) \\ &\sim \ (1 \pm \mathcal{A}' \cdot cos\vartheta) \end{aligned} \tag{2.83}$$

The integral asymmetry $\mathcal{A}'$ is proportional to $\wp_\mu \cdot \xi$ and depends on η in first and on δ in second order of x_0. Neglecting x_0 ($x_0 = 0$) one obtains

$$\mathcal{A}' \ = \ \tfrac{1}{3} \cdot \wp_\mu \cdot \xi \quad . \tag{2.84}$$

This allows one to determine ξ from an experiment using muons of known polarization. In the analysis the knowledge of the values of other muon decay parameters is unimportant.

The special case $\mathcal{A}(1) = \wp_\mu \cdot \xi\delta/\varrho$ has been the basis of a null-experiment for

a model independent precise absolute determination of the muon polarization $\wp_\mu$ and in turn of the ν_μ polarization, $\wp_{\nu_\mu}$, as well as for a determination of $\xi\delta/\varrho$. Suppose positive muons from the decay of π^+ at rest, $\pi^+ \rightarrow \mu^+\nu_\mu$ are investigated. The μ^+ helicity then is equal to the ν_μ helicity h_{ν_μ}, which is known to be negative. These muons then are polarized with spins opposite to their line of flight with $\wp_\mu = |\wp_{\nu_\mu}|$. From Eq. 2.80 we find

$$w(1,\vartheta) \sim (1 + \wp_\mu \cdot (\xi\delta/\varrho) \cdot cos\vartheta) \quad , \tag{2.85}$$

where ϑ is again the angle between the polarization of the muon and its decay positron. With the standard model values $\wp_{\nu_\mu} = -1$ and $\xi\delta/\varrho = +1$, we conclude that a positive muon from a pion decaying at rest is forbidden to emit a positron of maximum energy exactly along its line of flight ($\vartheta = 180^0$). This has been the basis of an ingenious precision experiment by the LBL-Berkeley-Northwestern-Triumf collaboration [60, 36] (see Fig 2.4).

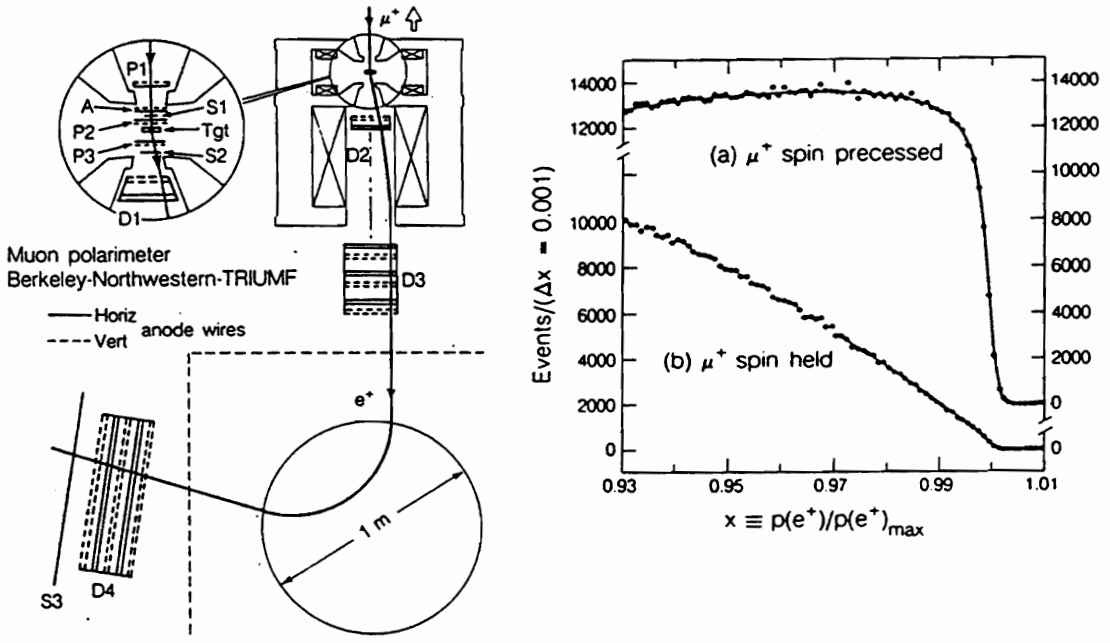

Fig. 2.4 Left: Positron momentum spectrometer. Positive muons fully backward polarized stop at "Tgt", where their spins either are kept fixed in a longitudinal holding field or where they precess in a transverse field. **Right:** Positive muons *do not* emit positrons of maximum energy along the direction opposite to their spins. This is demonstrated by curve (b) at $x = 1$. Curve (a) confirms that muons with isotropically distributed spins *do* emit positrons at $x = 1$. From Ref. [28].

The experiment may be interpreted in an entirely model independent way as follows [27]:

Since w(1,0) is a non-negative number and since $\wp_\mu$ may take its maximum value $\wp_\mu = 1$ independently of $(\xi\delta/\varrho)$, we must have $|\xi\delta/\varrho| \leqq 1$. If an experiment using Eq. 2.85 yields the value $\mathcal{A}_{exp}$ for

$$\wp_\mu \cdot |\xi\delta/\varrho| \;=\; \mathcal{A}_{exp} \leqq 1 \quad , \tag{2.86}$$

then we can draw *two independent* conclusions:

$$|\xi\delta/\varrho| \;\geqq\; \mathcal{A}_{exp} \tag{2.87}$$

$$\wp_\mu \;\geqq\; \mathcal{A}_{exp} \qquad \Rightarrow \qquad |\wp_{\nu_\mu}| \;\geqq\; \mathcal{A}_{exp} \tag{2.88}$$

The art of the experiment is the design of an apparatus which selects undisturbed muons from pion or kaon decay and which then would yield a result of $\mathcal{A}_{exp}$ as close as possible to one. Then $\wp_\mu$, $|\wp_{\nu_\mu}|$, and $|\xi\delta/\varrho|$ would be constrained between $\mathcal{A}_{exp}$ and one.

Beams of muons with a precisely known relation between the polarization $\wp_\mu$ and $\wp_{\nu_\mu}$ are produced by collecting those muons from pion or kaon decay $\pi^+ \rightarrow \mu^+\nu_\mu$ or $K^+ \rightarrow \mu^+\nu_\mu$, which have a unique recoil direction in space. This has been realized in two ways: as "surface muons" [61, 62, 63] and as muons from a parallel beam of pions decaying in flight in vacuum [64, 65, 66, 35].

Surface muons originate from pions (or kaons) decaying at rest just below the surface of the hadron production target. The recoil momentum pushes the muons out of this target into the direction opposite to the neutrino line of flight and possibly towards the ion optical beam transport system. The amount of their polarization equals $\wp_\mu = G \cdot |\wp_{\nu_\mu}|$, where the geometrical factor G is determined by the spread of the corresponding neutrino directions. G is estimated from Coulomb multiple scattering of the muons on their way out of the target. Values of $1-G \approx 10^{-3}$ with an uncertainty of roughly half of this size have been reached [60]. A great advantage of the surface muon beams is their small phase space which allows one to use small and thin stopping targets.

Muon beams from pions decaying in flight in vacuum avoid Coulomb multiple scattering. The muon spin lies in the plane of the laboratory lines of flight of the original pion, $\widehat{k}_\pi$, and its decay muon, $\widehat{k}_\mu$ and points inwards (towards $\widehat{k}_\pi$) for μ^+ and outwards for μ^- (See Fig. 2.5). The transverse and longitudinal muon spin components ζ_T and ζ_L with respect to the muon's laboratory line-of-flight are simply given by

$$\zeta_T \;=\; sin\vartheta_\mu / sin\Theta_\mu \tag{2.89}$$

$$\zeta_L \;=\; \mp\sqrt{1-\zeta_T^2}\,, \tag{2.90}$$

where the upper (lower) sign applies for the muon emitted with smaller (larger) momentum for the given angle of emission ϑ_μ, and where

ϑ_μ = laboratory angle between $\hat{k}_\pi$ and $\hat{k}_\mu$
Θ_μ = maximum laboratory angle by kinematics (Jacobian peak angle)
$sin\Theta_\mu = (m_\pi^2 + m_\mu^2)/(2m_\pi k_\pi)$
k_π = pion beam momentum.

The selection of a small slice of muon energy in the laboratory in the vicinity of the Jacobian peak corresponds to a choice of a small range of neutrino directions and thus of a degree of polarization $\wp_\mu = G \cdot \wp_{\nu_\mu}$. Again, the geometrical factor G, which also has been studied experimentally [66], is close to one (> 0.99), and it is known with an uncertainty of $< 10^{-3}$ [35].

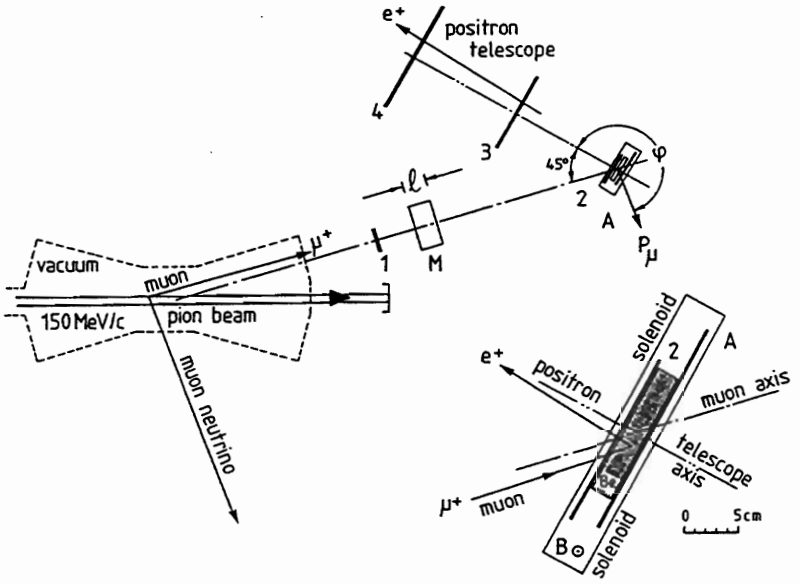

Fig. 2.5 Muon Spin Rotation apparatus to measure the integral asymmetry of the e^+ directional distribution following the decay of highly polarized muons. A parallel beam of monoenergetic (150 MeV/c) pions decay in flight in vacuum. Muons with energies within a well determined interval are selected to stop in a beryllium plate, Be, employing the moderator of length ℓ. The original orientation of the muons' polarization vector P_μ is thus defined. A rectangular solenoid produces a vertical magnetic field $B = 3\ mT$ causing the polarization of the stopped muons to precess in the horizontal plane. This gives rise to a sinusoidal modulation of the exponential decrease of the positron rate. The amplitude of the modulation ($\approx 1/3$) is proportional to the quantity desired, $P_\mu \xi$ [35].

In order to measure the decay asymmetry, the muons are stopped in a metal (Be, Al) immersed in a transverse magnetic field where the spins precess. Detectors follow the muon and the decay positron momenta. The positron intensity shows a time modulation corresponding to the decay asymmetry. It is a favourable circumstance that there exist substances (Al, Cu, Ag, Au, bromoform) that barely influence the spin direction of muons which reside inside of them or which they do slow down. The disappearance of muon polarization during slowing down [67, 68] and thermalization [69], i.e. at early times compared to the muon precession time, fakes a smaller $\mathcal{A}_{exp}$. Depolarization at later times is seen in the data [70, 36]. This "muon spin relaxation" is a central subject of "μSR spectroscopy" [71]. It is a complicated solid state phenomenon whose time dependence cannot be reliably predicted with high precision. It can be accounted for essentially by extrapolation of the precession signal amplitude to zero time. The determination of the parameters of the extrapolating function in the same experiment generally reduces the statistical significance of the data considerably due to their strong correlation with the signal. The relaxation time in pure metals at room temperature is often conveniently big compared to the muon lifetime (See Fig. 2.6). For the measurement of $\wp_\mu \xi\delta/\varrho$, and of δ a precise positron energy spectrometer with well known resolution (0.15% rms) and acceptance has been used [36]. The results are

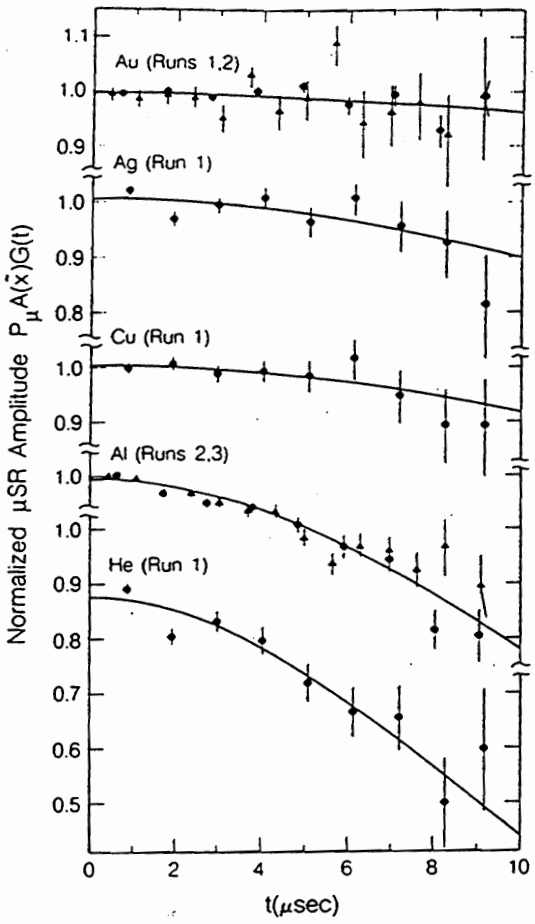

Fig. 2.6 Decay of the precession signal amplitude due to loss of phase coherence between the rotating muon spins. The curves assume a Gaussian time dependence of the relaxation [70]. Data obtained with the apparatus of Fig. 2.4.

$$\delta = (748.6 \pm 2.6_{\text{stat.}} \pm 2.8_{\text{syst.}}) \times 10^{-3}$$

$$\wp_\mu \xi\delta/\varrho = (997.90 \pm 0.46_{\text{stat.}} \pm 0.75_{\text{syst.}}) \times 10^{-3}$$

$$\text{and } \wp_\mu \xi\delta/\varrho > 996.82 \times 10^{-3} \ (90\% \ c.\ell.)$$

With Exprs. 2.86-2.88:

$$\begin{aligned} \wp_\mu &> 996.82 \times 10^{-3} \text{ (90\% } c.\ell.\text{)} \\ \wp_{\nu_\mu} &> 996.82 \times 10^{-3} \text{ (90\% } c.\ell.\text{)} \\ |\xi\delta/\varrho| &> 996.82 \times 10^{-3} \text{ (90\% } c.\ell.\text{)} \end{aligned}$$

For the measurement of $\wp_\mu \cdot \xi$, positron detectors with low energy thresholds are used. The results obtained from the decays $\pi^+ \to \mu^+\nu_\mu$ ($\wp_\mu^\pi$) and $K^+ \to \mu^+\nu_\mu$ ($\wp_\mu^K$) are:

$$\begin{aligned} \wp_\mu^\pi \cdot \xi &= (1002.7 \pm 7.9_{\text{stat.}} \pm 3.0_{\text{syst.}}) \times 10^{-3} \text{ [35]} \\ \wp_\mu^K \cdot \xi &= (1001.3 \pm 3.0_{\text{stat.}} \pm 5.3_{\text{syst.}}) \times 10^{-3} \text{ [37]} \\ \wp_\mu^K \cdot \xi &> 990 \times 10^{-3} \text{ (90\% } c.\ell.\text{) [37]} \end{aligned}$$

Since ξ is not limited close to the measured value of $\wp_\mu \cdot \xi$, we cannot draw any specific conclusion on $\wp_\mu$ and ξ separately, contrary to the case of $\wp_\mu\xi\delta/\varrho$. In fact, $-3 \leqq \xi \leqq +3$, and thus the authors of ref. [35] do not quote an upper limit on $\wp_\mu\xi$. In order to isolate ξ from $\wp_\mu\xi$, one has to deduce $\wp_\mu$ from the measurement of $\wp_\mu\xi\delta/\varrho$ of ref. [36]. Examples of experimental data from the most simple apparatus (Fig. 2.5) as well as from the most sophisticated one (Fig. 2.4) are shown in Figs. 2.7 and 2.8.

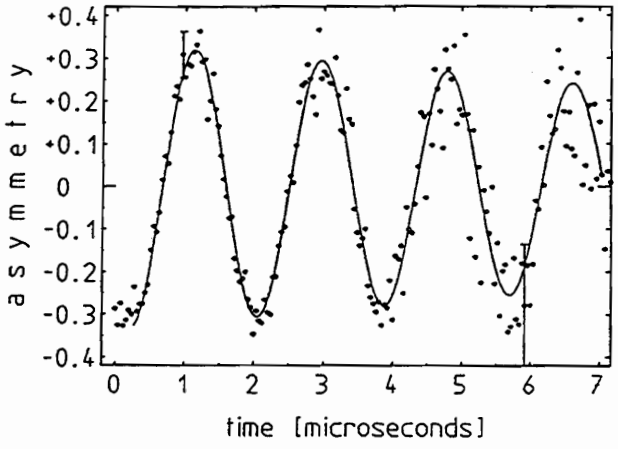

Fig. 2.7 Measured time distribution between the stop of highly polarized μ^+ in Be and the observation of the decay positron [35, 66]. Data obtained with the apparatus of Fig. 2.5. Positrons from a low threshold up to the maximum energy have been accepted. The exponential μ decay time has been factored out. The spatial asymmetry of the emitted e^+ relative to the muon spin rotates due to the spin's precession in a weak magnetic field. This generates the oscillation of the time spectrum. The solid line is the result of a best fit to the data. The slow decrease in amplitude (relaxation) is due to internal fields in Be.

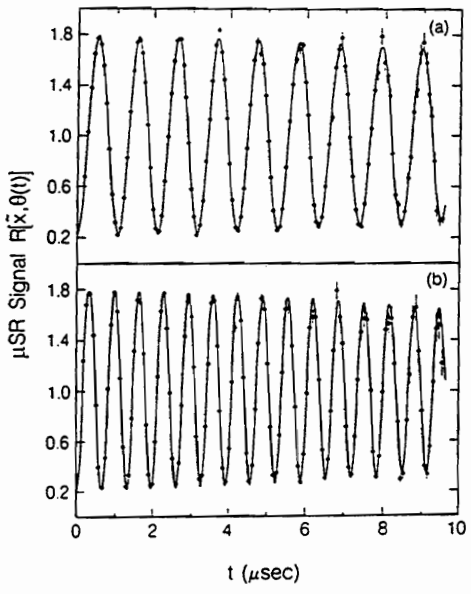

For the $\wp_\mu \xi$ experiments (e.g. Fig. 2.7 or Ref. [37]) it is typical that corrections are small. The raw data show an amplitude, which is close to the final experimental result. These experiments also constitute a simple means to measure $\wp_\mu$.

Fig. 2.8 Measured distributions of the time intervals between the stop of highly polarized and precessing muons in very pure metals and the acceptance of the decay positron [70]. In this experiment only the positrons of highest momentum are selected which results in a large asymmetry. Curve (a) has been taken at a field of 7 mT, curve (b) at 11 mT. The exponential decay time has been factored out. Data obtained with the apparatus of Fig. 2.4.

Fig. 2.9 shows that the measured decay asymmetry, as derived from data similar to those of Fig. 2.8 but with positrons selected at various momenta, vanishes near $x = 0.5$. The small but finite shift $(x_\delta - 0.5)$ is a result of radiative corrections to the decay spectrum of Eq. 2.4.

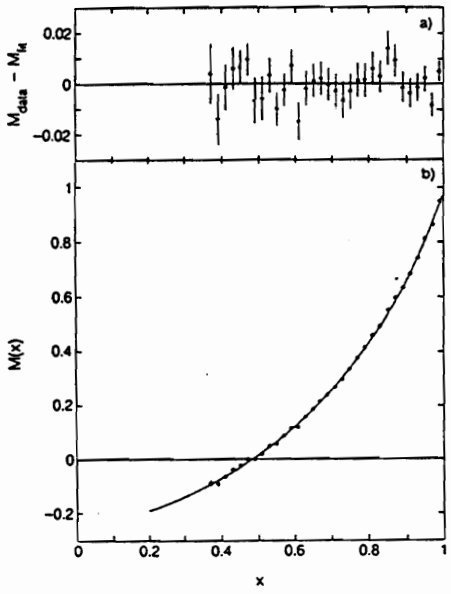

Fig. 2.9 Decay asymmetry of e^+ from μ^+ decay as a function of the reduced positron energy [28]. The curve is a fit to the theory with internal radiative corrections. The upper plot shows the statistical errors and fit residuals for the 32 data points. Data obtained with the apparatus of Fig. 2.4.

The result of Ref. [36] is of importance in several respects:

(1) It constitutes by far the best measurement of the magnitude of a neutrino polarization, in particular of $\wp_{\nu_\mu}$ [27]. The sign of $\wp_{\nu_\mu}$ has been measured in separate experiments [72]- [77].

(2) Surface muon beams from pion decay can be prepared with a high and well known polarization $\wp_\mu > 0.99682$ (90% $c.\ell.$)

(3) The polarization $\wp_\mu$ of muons stopped in various metals is preserved to a high accuracy during several lifetimes under the influence of an external magnetic holding field of 1.1 T [60] or 0.3 T [36].

(4) The precise value of $\xi\delta/\varrho$ gives the strongest constraint for the absence of couplings with both right-handed electrons and muons, g^V_{RR} and g^S_{RR}. Together with δ and ϱ, it constrains g^γ_{LR} , $\gamma = S, V, T$.

(5) The product $\wp_\mu\xi\delta/\varrho$ is of interest in the search for right-handed currents introduced to models which include also the pion (or kaon) decay.

For the theoretical significance of the results we refer to Refs. [17, 78, 79, 80, 81]. We restrict ourselves to mentioning two special cases of left-right symmetric models which have been used to interpret experimental results.

Right-handed currents admixed to the interaction change $\mathcal{A}_{exp}$, because the decay muon is no more fully polarized ($\wp_\mu < 1$) and because high energy positron emission opposite to the muon spin is no more strictly forbidden ($\xi\delta/\varrho < 1$, $\xi < 1$). Such a deviation from the standard model may e.g. be due to a right-handed intermediate vector boson W_R of mass $\approx m_R$. With the assumption of left-right symmetry, the parity violation of weak interactions at low energies would still be preserved, if $m_R \gg m_L$. We now expect $g^V_{RR} \neq 0$ dependent on m_R, and $g^V_{RL} \neq 0$, $g^V_{LR} \neq 0$ dependent on a possible mixing of the states W_R and W_L. In such a model in which $g^V_{RL} = g^V_{LR}$ and in which all of the scalar and tensor couplings are zero and therefore also $c = c' = a' = 0$ we find

$$(1 - \xi\delta/\varrho) \approx 2|g^V_{RR}|^2 \quad . \tag{2.91}$$

and

$$(1 - \xi) = 2|g^V_{RR}|^2 + 2|g^V_{RL}|^2 \tag{2.92}$$

The relations of the coupling constants $g^V_{\epsilon\mu}$ to the model parameters $\varepsilon = (m_L/m_R)^2$ and the $W_R - W_L$ mixing angle ζ are:

$$g^V_{LL} \approx 1 \tag{2.93}$$

$$g^V_{RR} \approx \varepsilon \ll 1 \tag{2.94}$$

$$g^V_{RL} = g^V_{LR} \approx \zeta \ll 1 \quad . \tag{2.95}$$

Right-handed currents decrease the muon polarization in kaon decay more strongly than in pion decay if the right-handed quarks mix more than the usual left-handed ones, i.e. if $\vartheta_R > \vartheta_L$ [82]. The measurement of $\wp_\mu\xi$ with muons from $K^+ \rightarrow \mu^+\nu_\mu$ may thus be somewhat more sensitive to ε in this case. (We use

$\vartheta_R \equiv \theta_1^R, \vartheta_L \equiv \theta_1^L$ and $\theta_3^R = \theta_3^L = 0$, where $\theta_i^\varepsilon, i = 1,3$, $\varepsilon = R, L$ is the notation of ref. [82]).

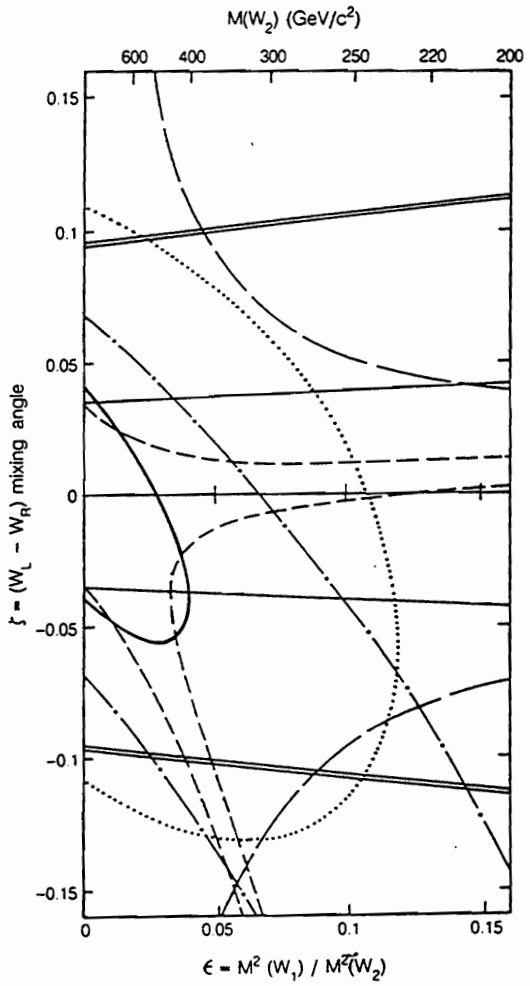

Fig. 2.10 Experimental 90% confidence limits on the mass-squared ratio ε and mixing angle ζ for the gauge bosons W_R and W_L [36]. The allowed regions include $\varepsilon = \zeta = 0$. Bold curve from $\wp_\mu \xi\delta/\varrho$ [36], dotted curve from $\wp_\mu \xi = (972 \pm 14) \times 10^{-3}$ as of 1968, solid lines from ϱ [59], double lines from νN and $\bar{\nu} N$ scattering [83]. Other curves from nuclear β decay. For more details, see Ref. [36].

Table 2.3 summarizes the basic relations. LRS1 is the special case $\vartheta_L = \vartheta_R$ of LRS2, as described in Ref. [17] but with equal strengths $g_R = g_L$ and CP conservation $\omega = \alpha = 0$. A measured value of $\varrho, \xi, \wp_\mu$ or some combination defines a contour plot in the plane of ε vs. ζ. If it is compatible with the standard model value, its error places limits on m_R and on the mixing angle (See Fig. 2.10). In the strangeness changing decay $K^+ \to \mu^+ \nu_\mu$ the quark mixing angle enters as $sin\vartheta_R$, in $\pi^+ \to \mu^+ \nu_\mu$ as $cos\vartheta_R$. With the usual assumption that the muons from kaon and from pion decay are identical, the difference $\vartheta_R \neq \vartheta_L$ just leads to a different muon polarization $\wp_\mu$.

Since most of the muon decay experiments do not observe the identity of the neutrinos, the decay $\mu^+ \to e^+ \tilde{\bar{\nu}}_\mu \tilde{\nu}_e$ to the supersymmetric scalar partners of the neutrinos, mediated by a wino, may admix positrons with deviating properties [84, 85]. These influence the measured values of ξ, δ and ϱ but leave $\xi\delta/\varrho$ unchanged. Under the assumption of light scalar neutrinos ($m_{\tilde{\nu}} < 10\ MeV$) which would not energetically inhibit the decay, the sensitivities to a hypothetical wino of mass $\tilde{m}$ are also given in Table 2.3. We note that a supersymmetric contribution is not the result of a four-fermion interaction. In general, the expressions derived from Eq. 2.1 then do not provide the correct degrees of freedom for the corresponding observables [4]. Some results are (90% *c.l.*): $m_R > 482\ GeV/c^2$ ($\zeta = 0$), $|\zeta| < 0.040$ ($m_R = \infty$) [36]; $m_R > 635\ GeV/c^2$ ($\zeta = 0, \sin\vartheta_R = 1$) [37]; $\tilde{m} > 270\ GeV/c^2$ (light sneutrinos) [35]. For limits on composite leptons and on familons, see Ref. [36].

Table 2.3 Muon decay parameters beyond the standard model. $\varepsilon = (m_L/m_R)^2$, $\zeta = W_R - W_L$ mixing angle. The muon polarization also depends on the quark mixing angles ϑ_R *and* ϑ_L.
LRS1, LRS2: Left-right symmetric models [17, 78, 79, 80, 81, 82]
SUSY [84, 85]: $\lambda = (m_L/\,\widetilde{m})^2$. $\widetilde{m}$ = mass of the wino. Neutrino masses are assumed to be sufficiently small and of no influence on the energy spectrum.
The parametrization of other measurements may be read off this table immediately, e.g. $1 - |\wp_\mu \xi| \approx 1 - (1 - \wp_\mu) - (1 - |\xi|)$. Thus $1 - |\xi\delta/\varrho|$ becomes independent of λ.

Measurement	Standard Model	LRS1 $\vartheta_R = \vartheta_L$	LRS2 ϑ_L, ϑ_R	SUSY
$\frac{4}{3}(\varrho - \frac{3}{4})$	0	$-2\zeta^2$	$-2\zeta^2$	$\frac{1}{2}\lambda$
$\frac{4}{3}(\delta - \frac{3}{4})$	0	0	0	$-\frac{3}{2}\lambda$
$1 - \lvert\xi\rvert$	0	$2(\varepsilon^2 + \zeta^2)$	$2(\varepsilon^2 + \zeta^2)$	-2λ
$1 - \wp_\mu$	0	$2(\varepsilon + \zeta)^2$		
$1 - \wp_\mu^\pi$	0		$2(\varepsilon \cdot \frac{cos\vartheta_R}{cos\vartheta_L} + \zeta)^2$	
$1 - \wp_\mu^K$	0		$2(\varepsilon \cdot \frac{sin\vartheta_R}{sin\vartheta_L} + \zeta)^2$	

2.4.4. Longitudinal Electron Polarization

The measurement of the longitudinal polarization P_L of the electrons from the decay of polarized or unpolarized muons allows one to determine the parameters ξ'' and ξ', as can be seen from Eqs. 2.9, 2.10, 2.21 and 2.22. The parameter ξ' is of special interest. In terms of the coupling constants $g^\gamma_{\varepsilon\mu}$ we have

$$\begin{aligned} 1 - \xi' &= \tfrac{1}{2}(4 \cdot (|g^V_{RR}|^2 + |g^V_{RL}|^2) + |g^S_{RR}|^2 + |g^S_{RL}|^2 + 12 \cdot |g^T_{RL}|^2) \\ &= 2(Q_{RR} + Q_{RL}) \equiv 2Q^e_R \quad , \end{aligned} \tag{2.96}$$

where $Q_{\varepsilon\mu}$ is the probability of the decay of a muon with chirality μ into an electron with chirality ε. Note that Eq. 2.96 is a sum of absolute squares where only coupling constants with $\varepsilon = R$ appear. A deviation of ξ' from 1 would require the existence of a coupling with the right-handed components of the electron, i.e. at least one $g^\gamma_{R\mu} \neq 0$. Conversely, a measurement with the result $\xi' = 1$ proves that the coupling acts exclusively on the left-handed component of the electron.

To determine ξ', the longitudinal polarization P_L of the electrons from unpolarized muons has been measured. For the purpose of illustration, we neglect the electron mass m_e and use the experimentally well confirmed values $\varrho = \delta = \frac{3}{4}$ and obtain from Eq. 2.9

$$\xi' = P_L \quad .$$

The measurement of the electron's longitudinal polarization P_L consists of its comparison with the spin polarization of the electrons contained in a piece of saturated ferromagnetic material [86]-[95], [67]. The comparison is done by scattering

the decay electrons from the electrons of a ferromagnet, using the fact that relativistic electron-electron scattering most often occurs when the two spins have opposite directions. See Fig. 2.11.

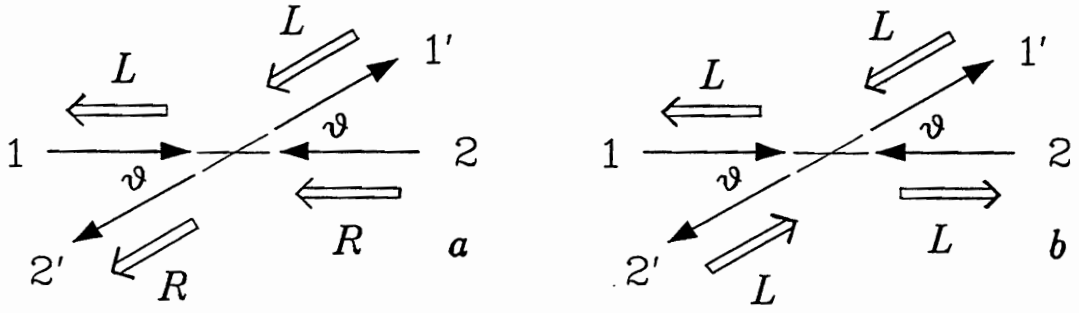

Fig 2.11 Comparison of the longitudinal polarizations of electrons 1 and 2.
Scattering of two fast electrons $1 + 2 \rightarrow 1' + 2'$ occurs most often when the spins look opposite, as in *case b*. In scattering due to a vector interaction (such as electromagnetic), *chirality* R, L is conserved. In case of *relativistic* particles, this means, that 1 and $1'$, and also 2 and $2'$ have the same *helicity*. Angular momentum conservation partially inhibits the polarization configuration $LR \rightarrow LR$ (*case a*) mainly for big scattering angles ϑ, whereas it is of no influence for the configuration $LL \rightarrow LL$, (*case b*). The $LL \rightarrow LL$ configuration is furthermore favoured by the fact, that the *indistinguished* reaction $1 + 2 \rightarrow 2' + 1'$ leads to *distinguishable* and thus incoherent final states in *case a*, but to *indistinquishable* and thus coherent final states in *case b*. For $\vartheta = 90^0$ e.g. LL is *eight* times more probable. The same conclusion applies, when particle 1 is a relativistic positron, which scatters elastically from an electron. The annihilation in flight $e^+e^- \rightarrow \gamma\gamma$ of relativistic positrons with electrons, however, occurs mainly when their longitudinal spins are parallel (RL).

The spin polarization of the ferromagnet's electrons is deduced from their total spin angular momentum, which becomes macroscopically measurable, when all electron spins are flipped simultaneously, as done in Einstein-de Haas experiments. For the comparison of the longitudinal polarization of *positrons* from $\mu^+ \rightarrow \bar{\nu}_\mu e^+ \nu_e$ with the polarization of a ferromagnet's electrons, elastic scattering as well as annihilation in flight into two gamma rays, $e^+e^- \rightarrow \gamma\gamma$, are most suitable. The results of measurements of P_L are displayed in Fig. 2.12. They yield an average of $< |P_L| > = 0.998 \pm 0.042$. Radiative corrections to the electron polarization $\vec{\varphi}_e$ are negligibly small [96, 97].

From the resulting error of ξ', which is dominated by the error of this $< |P_L| >$, upper limits for all couplings of right-handed *electrons* to muons (of any handedness) $|g^\gamma_{R\mu}|$, $\mu = R, L$, follow, in principle, from Eq. 2.96. Improved

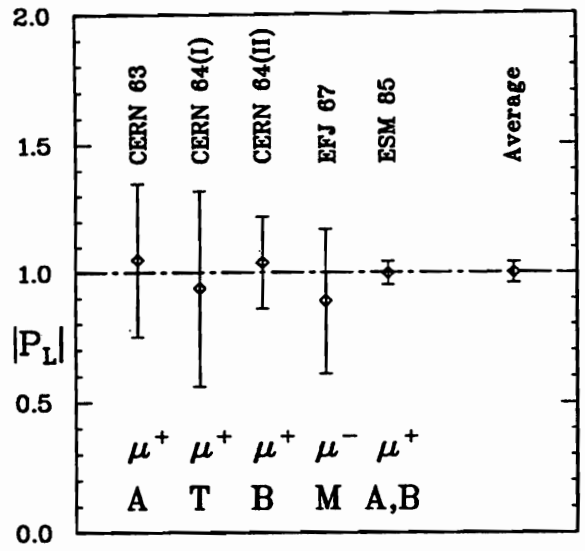

Fig. 2.12 Longitudinal polarization of electrons and positrons in the decay of unpolarized muons. The experiments (CERN 63 [98], CERN 64(I)[99], CERN 64(II)[100], EFJ 67[101], ESM 85[34]) confirm full forward polarization for positrons and full backward polarization for electrons, i.e. weak coupling to *left-handed* electrons only.
A (Annihilation), T (Transmission of polarization in bremsstrahlung), B (Bhabha scattering), and M (Møller scattering) indicate the methods used to compare the decay particle's polarization with the electron polarization in a ferromagnet.

values of these limits are obtained for $|g^V_{RL}|$ and $|g^S_{RL} + 6g^T_{RL}|$ by considering also

$$B_{RL} = \tfrac{1}{16}|g^S_{RL} + 6g^T_{RL}|^2 + |g^V_{RL}|^2 = \tfrac{1}{2A}(a + a') \quad . \tag{2.97}$$

For all couplings of right-handed *muons* to electrons (of any handedness) $|g^\gamma_{\varepsilon R}|$, $\varepsilon = R, L$, better limits have been reached from the experiments with polarized muons.

The parameter ξ'' in positive muon decay has been determined from a measurement of $P_L(x, \vartheta)$ as a function of the positron reduced energy x and the angle ϑ between the muon spin and the positron momentum [34]. The present precision of the measured combination $(\xi'' - \xi \cdot \xi')/\xi = -0.35 \pm 0.33$ does, however, not lead to better constraints of the couplings.

Experiments measuring P_L and $P_L(x, \vartheta)$ are described in Fig. 2.13. Positive pions decay inside the stopping target, where they create unpolarized muons, which also decay. The positrons encounter the electrons of the magnetized iron foil. Both effects, elastic scattering ($e^+e^- \to e^+e^-$) or annihilation in flight ($e^+e^- \to \gamma\gamma$) are observed in order to quantitatively compare the positron polarization with the spin polarization of the electrons in the ferromagnet. The four NaI counters identify and measure the energies of the final state particles e^+e^- or $\gamma\gamma$. The apparatus thus performs simultaneously two independent experiments, one is most sensitive to antiparallel, the other to parallel spins. The backgrounds and the sources of the systematic errors are widely different in the two cases. Since the multiple scattering in the iron foil alters the directions of flight of the charged particles, but leaves their energies mostly unchanged, the measured energies allow the determi-

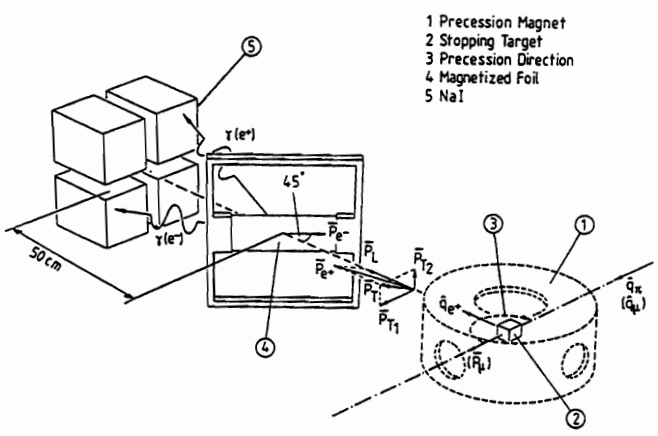

Fig. 2.13 Measurement of the longitudinal polarization of positrons from polarized and unpolarized muons. Longitudinally polarized muons stop at 2 and precess. (For unpolarized muons, pions stop at 2 and the magnet is removed). The decay positron scatters or annihilates at 4. e^+e^- or $\gamma\gamma$ pairs are detected at 5. From Ref. [34]

nation of the energy of the incoming decay positron and of the polarization sensitivity of the cross section. For both reactions the cross section has the form

$$\sigma_i(E_1, E_2) = \sigma_{oi}(E_1, E_2) \cdot [1 + A_i(E_1, E_2) \cdot \vec{\wp}_{e^+} \cdot \vec{\wp}_{e^-}] \quad , \tag{2.98}$$

where i stands for $(e^+e^- \to e^+e^-)$ or $(e^+e^- \to \gamma\gamma)$. E_1 and E_2 are the laboratory energies of the final state particles. $\vec{\wp}_{e^+}$ and $\vec{\wp}_{e^-}$ are the polarizations to be compared. Since $\vec{\wp}_{e^-}$ lies in the plane of the foil, as does the magnetization, the foil is inclined (under 45^0) to the positron's line of flight.

The analyzing power $\mathcal{A}_i(E_1, E_2)$ reaches high values (-0.78 for scattering and +0.89 for annihilation), however the fraction of electrons which take part in ferromagnetism is small. $\wp_{e^-}$ has typical values of 55×10^{-3}. Therefore, upon changing the foil inclination from 45^0 to 135^0 or reversing $\vec{\wp}_{e^-}$, correspondigly small signals in $\sigma_i(E_1, E_2)$ arise.

$\wp_{e^-}$ is determined from the macroscopic gyromagnetic ratio g' of iron as deduced from the angular momentum an iron piece displays when its magnetization is reversed. The electrons in iron may contribute to the magnetization and to the angular momentum with a gyromagnetic ratio $g = 2$, when they are polarized, and with $g = 1$, when they perform an orbital motion. Unpolarized electrons at rest contribute to neither of them. For pure iron the Einstein-De Haas effect gives $g' = 1.919 \pm 0.002$ [102]. This result, being not far from the free electron's g value shows that most of the magnetization comes from the polarized electrons, namely $f \equiv$ (magnetization due to spin orientation) / (total magnetization) = $(1-1/g')/(1-1/g) = 0.958 \pm 0.001$. From the measured magnetization $M \approx B/\mu_0$ the electron polarization becomes

$$|\vec{\wp}_e| = \frac{f \cdot B}{\mu_0 \cdot N \cdot \mu_B} = (54.44 \pm 0.56) \times 10^{-3}, \tag{2.99}$$

where N is the number density of electrons in iron and μ_B the Bohr magneton.

In order to measure the longitudinal polarization $P_L(x, \vartheta)$ also as a function of the angle ϑ between the muon spin and the electron momentum, *polarized muons* are stopped in the stopping target of Fig. 2.13. Due to a vertical magnetic field in the target region, they precess in a horizontal plane. A counter telescope, not shown in Fig. 2.13, detects their precession phase. From the individual decay times the angle ϑ is known for each recorded event.

With the experimental techniques available today and with considerable effort in instrumentation and beamtime, only moderate improvements (factor 3, say) in the polarization results seem possible. The small effective analyzing powers and their absolute calibration are a difficulty.

2.4.5. Transverse Electron Polarization

Transverse electron polarization P_T (P_{T_1}, P_{T_2}) is defined in Fig. 2.1. Independent of any assumption about the mechanism of muon decay or even the nature of the two unobserved neutral particles, time reversal invariance (disregarding the negligible final state interactions) requires $P_{T_2} = 0$.

In a decay into light photinos, $\mu \to e\tilde{\gamma}\tilde{\gamma}$, P_T of observable size may arise, if the two effective masses $\mathcal{M}_k$, $k = R, L$, of the intermediate scalar leptons are not too heavy: $|\mathcal{M}_L| \cdot |\mathcal{M}_R| \gtrapprox 4m_W^2$ (90% *c.ℓ.*) [103, 32].

Within the four fermion interaction Eq. 2.1 the measurement of $\vec{P}_T$ as a function of energy allows one to determine the parameters $\eta \equiv (\alpha - 2\beta)/A$, $\eta'' \equiv (3\alpha + 2\beta)/A$, α' and β' (see Eqs. 2.13, 2.14, 2.19 and 2.20). η is of special interest. Although η describes, together with the Michel parameter ϱ, the shape of the (isotropic) positron energy spectrum, it is practically difficult to deduce its value from a spectrum measurement, since its influence there is suppressed by a factor $x_0 \approx 10^{-2}$. On the other hand, its value has to be known for a precise determination of ϱ, since η and ϱ are statistically highly correlated. In Eq. 2.19 for P_{T_1}, η arises without suppression factor. It is interesting to note that P_{T_1} does not vanish in the standard model interaction, as may be seen from Eq. 2.13, and it may take sizeable values ($|P_{T_1}| \leqq 1/3$) for positron energies $E_e <$ few times m_e. The parameters α' and β' determine P_{T_2}.

Since, by definition, probabilities and polarizations cannot exceed unity, there exist bounds such as Exprs. 2.46-2.51. From 2.49 and 2.50 we deduce

$$\alpha^2 + \alpha'^2 \leqq (a - a') \cdot (a + a') \tag{2.100}$$

$$\beta^2 + \beta'^2 \leqq (b - b') \cdot (b + b') \quad . \tag{2.101}$$

The values of the factors on the r.h.s., as obtained from the precision measurements of ξ', $\xi\delta/\varrho$, ξ, δ (or ϱ), are small, except for $(b - b')$, which is of order $A/2 = 8$. At present, both products on the r.h.s. are below the experimental uncertainties of α, α', β and β' whose values are compatible with zero. They vanish, if ξ' takes

the standard model value, $\xi' = 1$.

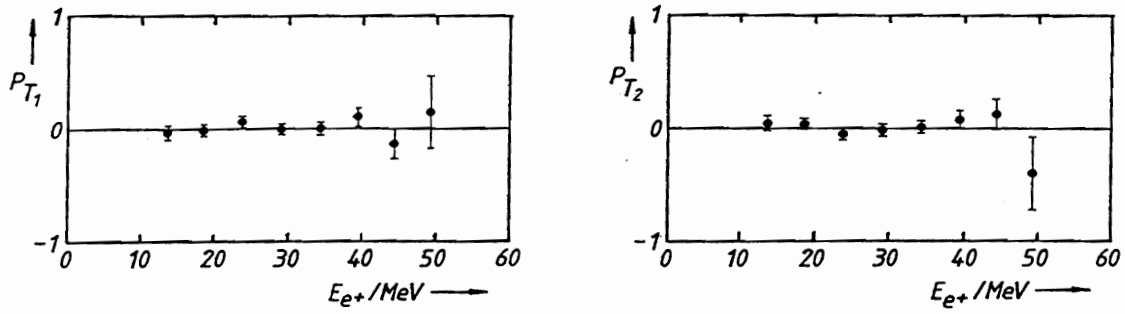

Fig. 2.14 The transverse polarization components P_{T_1} and P_{T_2} as obtained from an analysis of the annihilation in flight events as a function of the positron total energy E_{e^+}. The errors include both statistical and systematic contributions. Data obtained from the apparatus of Fig. 2.15. From Ref. [32].

The experimental results are displayed in Fig. 2.14. They are compatible with being independent of the energy between 9.5 MeV and maximum positron energy. The averages over the energy are

$$P_{T_1} = (16 \pm 23) \times 10^{-3}$$
$$P_{T_2} = (\ 7 \pm 23) \times 10^{-3}$$

The values of $\alpha, \alpha', \beta, \beta'$ are collected in Table 2.4.

Table 2.4 Results for α/A, α'/A, β/A, β'/A, η and η'' from the experiment of Fig. 2.15. The errors are dominated by statistics. A value of zero for a parameter indicates that it was set identically equal to zero in the least squares analysis. Also included are the low energy shape parameter $\eta = (\alpha - 2\beta)/A$ and the parameter $\eta'' = (3\alpha + 2\beta)/A$. Their errors include the correlation between α/A and β/A. The correlation coefficient between α/A and β/A (or α'/A and β'/A) is $\rho = -0.894$. All other correlation coefficients are ≈ 0. In all cases, the χ^2 per degree of freedom was 0.97. (All values are given in units of 10^{-3}). From Ref. [32].

α/A	β/A	α'/A	β'/A	η	η''
15 ± 52	2 ± 18	−47 ± 52	17 ± 18	11 ± 85	48 ± 125
0	6 ± 8	0	3 ± 8	−12 ± 16	12 ± 16
19 ± 23	0	−1 ± 23	0	19 ± 23	58 ± 70
16 ± 52	2 ± 18	0	0	13 ± 85	51 ± 125
0	0	−46 ± 52	16 ± 18	0	0

From Eqns. 2.38, 2.39, 2.42 and 2.43 we see that α and α' are of second order in

deviations from the standard model, whereas

$$\begin{aligned} \beta &= -4Re\left\{g_{RR}^{V}g_{LL}^{S*} + g_{LL}^{V}g_{RR}^{S*}\right\} \\ \beta' &= 4Im\left\{g_{RR}^{V}g_{LL}^{S*} - g_{LL}^{V}g_{RR}^{S*}\right\} \end{aligned} \tag{2.102}$$

are sensitive to first order in (magnitude and phase of) g_{RR}^{S}.

The experiment is described in Fig. 2.15. It also consists of a comparison with the spin polarized electrons in a ferromagnetic foil, using annihilation in flight $e^+e^- \rightarrow \gamma\gamma$. It is based on the fact that the photons from the annihilation of a relativistic and transversely polarized positron electron pair are preferentially emitted in the plane spanned by the particle line of flight $\hat{q}_{e^+}$ and the bisector $\vec{b}$ between the (transverse) polarization directions $\vec{p}_T$ and $\vec{\varphi}_{e^-}$.

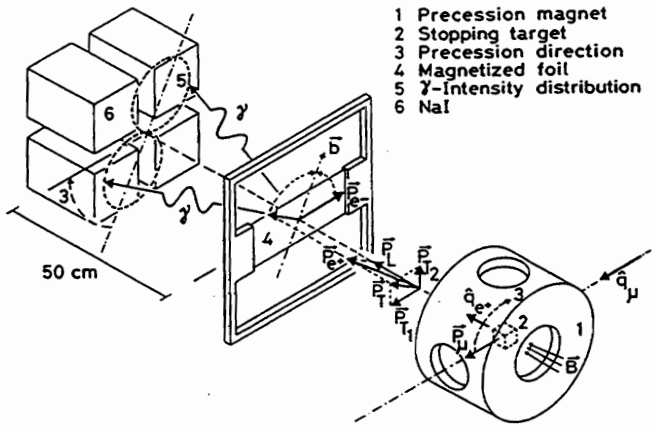

Fig. 2.15 Measurement of the transverse components P_{T_1} and P_{T_2} of the positron in muon decay. Longitudinally polarized muons at 2 precess in a vertical plane. The decay positrons annihilate with transversely polarized electrons at 4. The plane of the two annihilation gamma rays tends to contain the bisector $\vec{b}$ of the spin directions of the e^+e^- pair, as indicated by 5. The data are shown in Fig. 2.14. From Ref. [32].

The distribution as a function of the azimuthal angle φ between this plane and the actual plane of the two photons is given by

$$(d\sigma/d\Omega) \sim (1 - A_T(E_1, E_2) \cdot P_T \cdot \wp_{e^-} \cdot sin^2\varphi) \quad . \tag{2.103}$$

The polar diagram of this function is indicated in Fig. 2.15 as a "figure of eight". The analysing power $A_T(E_1, E_2)$ as a function of the photon energies E_1 and E_2 takes conveniently high values (up to 0.92), but $\wp_{e^-}$ is again small. P_T is measured by probing the above intensity distribution with the four NaI crystals detecting pairs of gamma rays. Instrumental asymmetries are averaged out by precessing the muon spins in a plane perpendicular to the symmetry axis of the apparatus. This causes the bisector $\vec{b}$ to precess with half of the muon spin rotation frequency. After a rotation of 180^0, however, the situation is identical for the detectors because of the two photons in the final state. Therefore the *effect* shows again the μSR frequency. In order to make use of the high intensity of the polarized muon beam at SIN (now PSI), the muon precession is synchronized to the arrivals of the

muon beam packets. This allows several muons to rotate with parallel spins in the stopping target at the same time.

The average positron direction of flight of the events detected by the non-diagonal NaI pairs is slightly off axis. Therefore the pair coincidence rate shows a small μSR modulation which marks the precession phase. For two NaI pairs of the same type (left and right or upper and lower pairs) this precession phase is shifted by 180^0, while for a signal due to a transverse polarization the phases are equal. From this one can deduce both magnitude and phase of $\vec{P}_T$ with respect to the muon spin. The data recorded for each event include information on the time of decay, on the positron's direction of flight and on the energies of the photons E_1 and E_2.

A finite positron transverse polarization would make the positron spins precess rapidly in the magnetic field in the target and tend to destroy itself. It is the Lorentz contraction of the magnet as seen by the positron which makes the time spent in the field sufficiently short.

2.4.6. Electron Neutrino Energy Spectrum

The shape parameter ω_L of the energy spectrum of left-handed ν_e from the decay of unpolarized μ^+ is completely analogous to the famous Michel parameter ϱ. There is an important difference, however: The standard model predicts $\varrho = 3/4$, but $\omega_L = 0$. This has intriguing consequences: As has been shown in Sect. 2.3.2 a precise measurement of ϱ in agreement with this prediction does not allow to derive any limits on six of the ten complex coupling constants describing muon decay. On the other hand a precise measurement of ω_L puts upper limits to the coupling constants $|g^S_{RR}|$, $|g^V_{LR}|$ and $|g^S_{RL} + 2g^T_{RL}|$ [22, 23].

From an experimental point of view it is exciting to realize that the measurement of ω_L is a null test of the standard model, comparable to the measurement of $P_\mu \xi\delta/\varrho$ [36] where one looks for events where none are predicted. For a purely left-handed (or a purely right-handed) interaction angular momentum conservation prohibits events at the maximum ν_e energy, while for all of the remaining interactions the rate is even enhanced at the spectrum endpoint. This leads to $\omega_L > 0$ and makes the method very sensitive (see Fig. 2.16).

The ν_e spectrum and therefore the parameter ω_L can be measured with a neutrino spectrometer of sufficient energy resolution and known energy dependence of the detection efficiency. One possible process is the reaction $^{12}C(\nu_e, e^-)^{12}N(g.s.)$ The KARMEN collaboration has built such a detector with 56 t liquid scintillator as target [38]. There, π^+ stop in a beam dump and decay into an unpolarized sample of μ^+. The μ^+ decay with a mean lifetime of 2.2 μs, and ν_e are converted promptly in the scintillator to e^-. The observation of the subsequent β^+ decay of $^{12}N(g.s.)$ with a mean lifetime of 15.9 ms, together with the required spatial co-

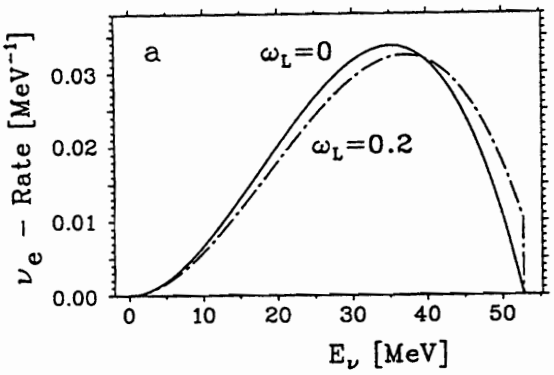

Fig. 2.16 Normalized energy distributions of left-handed ν_e from the decay of unpolarized μ^+. The spectrum shape parameter ω_L is the analog of the Michel parameter ϱ of the e^+. For a pure $V-A$ interaction ω_L is equal to zero. From Ref. [22].

Fig. 2.17. Sensitivity of the normalized energy distribution of e^- from the reaction $^{12}C(\nu_e, e^-)^{12}N(g.s.)$ to ω_L. The curves represent the product of the left-handed ν_e distribution of Fig. 2.16. with an absorption cross section σ_A parametrized by a polynomial of second order in the electron energy E_e. From Ref. [22].

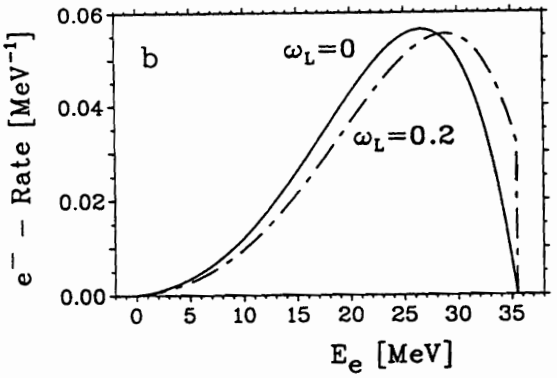

incidence, greatly reduces background (see Fig. 2.18). The authors assumed the pure $V-A$ law for the decay and obtained the energy dependence of the absorption cross section. They were able to measure the energy E_e of the e^- with the high precision $\sigma(E_e)/E_e = 11.5\%/\sqrt{E_e}$ (E_e in MeV). It has been pointed out recently that one can use the same measurement to derive independently the shape $d\Gamma_L/dy$ of the neutrino spectrum [22]. There it was shown that the pronounced structure at the spectrum endpoint for $\omega \neq 0$ can easily be separated from the smoothly varying absorption cross section σ_A. The sensitivity is further enhanced by the fact that σ_A rises strongly with energy, so that the region of interest is magnified as with a looking class (see Fig.2.17). This boosts the sensitivity to $\Delta\omega_L = 0.26/\sqrt{N}$, where N is the number of events.

In the following we assume that the KARMEN experiment will reach a final sensitivity of $\Delta\omega = 1\%$. This will improve existing upper limits to $|g^S_{RL} + 2g^T_{RL}|$ according to Eq. 2.25 [23]:

$$|g^S_{RL} + 2g^T_{RL}| \leqq \sqrt{\tfrac{16}{3}\Delta\omega_L} \tag{2.104}$$

The effects of contributions from right-handed ν_e lead to the effective spectrum shape parameter

$$\omega_{eff} = \frac{\omega_L Q_L^{\nu_e} + \varepsilon(y)\omega_R Q_R^{\nu_e}}{Q_L^{\nu_e} + \varepsilon(y) Q_R^{\nu_e}} \approx \omega_L + \varepsilon(y)\frac{Q_R^{\nu_e}}{Q_L^{\nu_e}}(\omega_R - \omega_L), \tag{2.105}$$

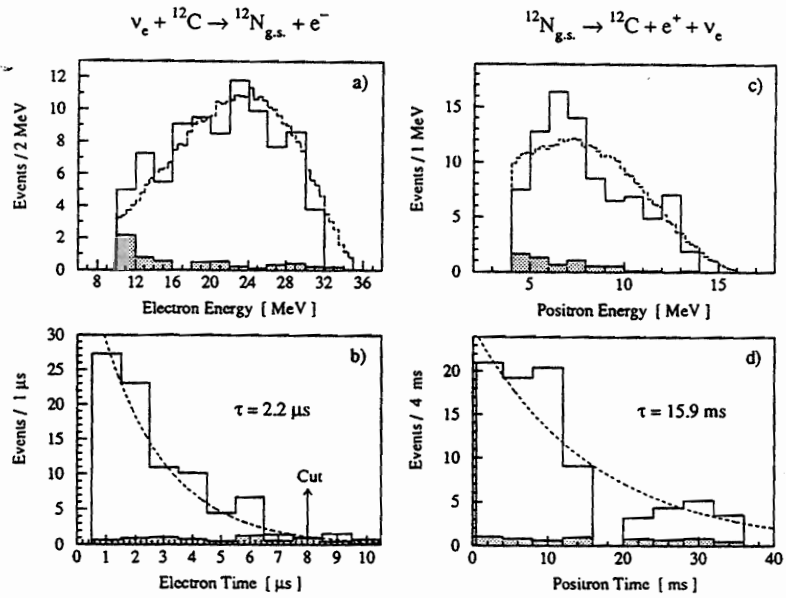

Fig. 2.18 Energy and time spectra of delayed coincidences from the reaction $^{12}C(\nu_e, e^-)^{12}N_{g.s.}$ and $^{12}N \rightarrow {}^{12}Ce^+\nu_e$. The visible energies of prompt electrons (a) and delayed positrons (c) are compared to simulations (broken lines). The corresponding time distributions are shown in (b) and (d) with the decay curves of μ^+ and ^{12}N superimposed. The normalized "beam off" background is shown as a shaded area. From Ref. [38].

where $\varepsilon(y)$ is the relative amount of right-handed ν_e contributing to the absorption cross section σ_A. From muon decay one finds that *emission* is suppressed by the factor $Q_R^{\nu_e}/Q_L^{\nu_e} < 0.087$ (90% *c.l.*), and from nuclear beta decay that *absorption* is suppressed by $\varepsilon(y) < 7.4 \times 10^{-3}$ (90% *c.l.*) [23]. The total contribution to the value of ω_L is therefore $< 0.6 \times 10^{-3}$ and can safely be neglected for the presently achievable precision.

The second observable of the neutrino distribution is the probability $Q_L^{\nu_e} = 1 - Q_R^{\nu_e}$ of the ν_e to be left-handed. A measurement of the total rate with an error of $< 5\%$ would improve present experimental limits which would lead to improved limits for the coupling $|g_{LL}^S|$, which can hardly be detected directly because both neutrinos are right-handed. The measurement of $Q_L^{\nu_e}$, however, does not seem to be feasible at present, mainly because the absorption cross section has to be determined absolutely either by theoretical calculation or by suitable calibration. The experimental error on the rate is presently in the order of 10% [38] and might be improved in a future, dedicated experiment.

2.4.7. Inverse Muon Decay

Measurements of inverse muon decay (IMD) are difficult to perform because a large ν_μ laboratory energy $E_{\nu_\mu} > 10.93\ GeV$ is transformed to the small c.m. energy $\sqrt{s} \approx \sqrt{2m_e E_{\nu_\mu}}$ resulting in extremely small cross sections. Thus in the CHARM II experiment [39] with its average neutrino energies of $\approx 20\ GeV$ the IMD total cross section is more than 1000 times smaller than the total neutrino

cross section on nucleons. The CCFR experiment [40] at the Fermilab Tevatron has used neutrinos with energies up to 600 GeV corresponding to a total energy of 780 MeV in the c.m. system. The three main problems in determining the absolute cross section precisely are, as usual, to identify the good events with well-known efficiency, to subtract correctly any background and to calibrate the neutrino flux with sufficient precision. For the identification kinematics is favourable because the small c.m. energy leads to events with correspondingly small transverse momenta and muon emission angles. Thus the trigger condition is given by single muons emitted nearly in forward direction and with negligible hadron energy. Although the background shapes cannot be reliably predicted, they should be equal for ν_μ and $\bar{\nu}_\mu$ reactions at $p_\perp^2 = 0$ [104]. Background comes from a broad continuum of quasi-elastic processes (QEP, charged current events on nuclei). The signal can be seen clearly as a narrow peak on the $p_\perp^2$ distribution over a huge broad background of QEP events (see Fig. 2.19). Since there is no IMD for $\bar{\nu}_\mu$ on e^- one uses the background for antineutrinos, properly

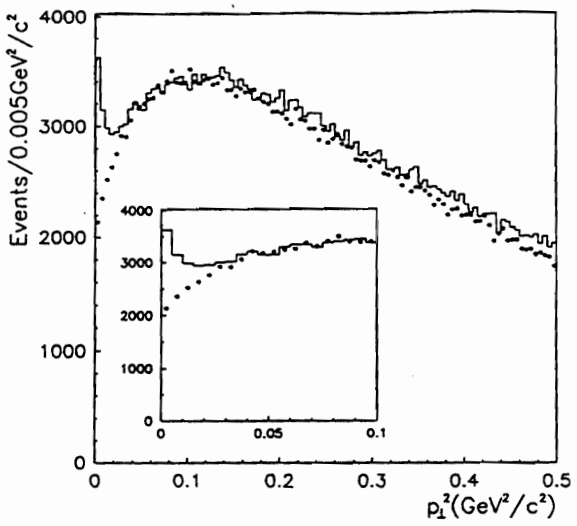

Fig. 2.19 $p_\perp^2$ distribution for events with $E_\mu > 10.9\ GeV$ and $E_{had} < 1.5\ GeV$ for incident ν_e (solid line) and $\bar{\nu}_\mu$ (marked with dots) [39]. The $\bar{\nu}_\mu$ distribution was normalized to the ν_e distribution in the range $0.05 < p_\perp^2 < 0.1\ GeV^2/c^2$. The insertion shows the small $p_\perp^2$ region with the peak due to the inverse muon decay reaction. From Ref. [39].

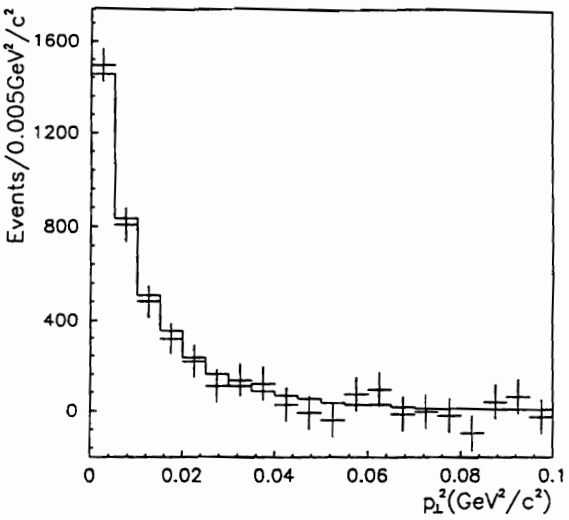

Fig. 2.20 Distribution of inverse muon decay experiments as a function of $p_\perp^2$ after subtraction of background. The solid line represents the expected distribution. From Ref. [39].

normalized, for background subtraction at small momentum transfer. The resulting IMD $p_\perp^2$ distribution agrees well with the expected distribution (see Fig. 2.20). For the CHARM II experiment the systematic error on the detection of the events is 4% and equal to the statistical error. The error on the total neutrino flux and therefore on the overall normalization is 5%. After subtracting radiative corrections, adding the errors in quadrature and dividing by the Born term of the standard model prediction they obtain

$$S = (1054 \pm 79) \times 10^{-3} \text{ [39]}$$

The result of the CCFR measurement, obtained at higher neutrino energies, is

$$S = (981 \pm 49_{\text{stat.}} \pm 30_{\text{syst.}}) \times 10^{-3} \text{ [40]}$$

These results tell how strongly left-handed ν_μ react with e^- and complete the informations from normal muon decay. They have enabled the first experimental confirmation of the assumptions of the standard model for muon decay [4].

2.4.8. Radiative Muon Decays

The measurement of the parameter $\bar{\eta}$ in the radiative decay, $\mu^+ \rightarrow \bar{\nu}_\mu e^+ \nu_e \gamma$, is of interest because it gives upper limits on $|g_{RL}^V|$, $|g_{LR}^V|$, $|g_{LR}^S + 2g_{LR}^T|$ and $|g_{RL}^S + 2g_{RL}^T|$. The branching ratio for this process, however,is only 1.4%, and a measurement has been performed as a by-product of searching for the process $\mu \rightarrow e\gamma$ [29, 105]. There e^+ and γ with energies $> 25\ MeV$ and at an angle of 180^0 were detected in coincidence. The decays of 6×10^{11} μ^+ resulted in the detection of only about 7500 events which yielded the value of $\bar{\eta} = -0.014 \pm 0.090$. We conclude that although an improved measurement of $\bar{\eta}$ is desirable, it seems to be rather difficult to reach a precision of, say, 0.01 which is necessary to be competitive with standard muon decay experiments.

The measurement of the decay $\mu^+ \rightarrow \bar{\nu}_\mu e^+ \nu_e e^+ e^-$ similarly is a by-product of the search for the decay $\mu \rightarrow 3e$ [31]. This experiment has verified the theoretically predicted branching ratio of $B = 36 \times 10^3$ and has determined limits for the probabilities $Q_{e\mu}$ and for B_{LR} and B_{RL} (see Sect. 2.2.4). With 2723 events the limits for Q_{RL} and B_{RL} are only a factor 3.3 less accurate than the limits from normal muon decay [31, 21], whereas Q_{RR} and Q_{LR} are by an order of magnitude less accurate. We conclude that a measurement of that decay is very useful due to its high sensitivity to the important decay parameters, but that the very low branching ratio makes it unrealistic to hope for improvements on the knowledge about the decay interaction from this particular decay.

3. Leptonic Tau Decays

3.1. General Remarks

The standard model considers the tau as a heavy muon or as a heavy electron, having its own associated neutrino. We discuss the experiments needed in order to prove that the tau (and its neutrino) shares the same weak interaction as the muon and the electron (and their neutrinos) do. We indicate to what extent the present experiments contribute to answer that question. For general reviews, see Refs. [10, 106, 107].

Leptonic τ decays shall be described by the same Hamiltonian and decay parameters as μ decay. They are insensitive to effects of the finite mass of the intermediate vector boson, since the lifetime and the decay parameters are modified by terms of the order of $(m_\tau/m_W)^2 \approx 0.5 \times 10^{-3}$ [108]. Effects of a finite τ-neutrino mass m_{ν_τ} are in the order of $m_{\nu_\tau}^2/m_\tau^2$ [109]. With the present experimental limit of $m_{\nu_\tau} < 31\ MeV/c^2$ [110, 111, 112] any possible effect is $\lessapprox 0.4 \times 10^{-3}$. Radiative corrections, however, do have to be taken into account in analyzing experimental results (See Ref. [15], [43]-[51]).

3.2. Universality

The universality of the charged weak interaction for the three leptonic decays $\mu \to \nu_\mu e \bar{\nu}_e$, $\tau \to \nu_\tau \mu \bar{\nu}_\mu$ and $\tau \to \nu_\tau e \bar{\nu}_e$ can be checked by testing whether

a) the couplings $g_{e\mu}^\gamma$ are equal and

b) the strength G_F is the same.

The Fermi constant G_F as the measure of the strength is given by [52]

$$G_F^2 = \frac{1}{\tau_\ell} \cdot \frac{192\pi^3}{m_\ell^5} \cdot \frac{1}{1 + 4\eta \cdot m_{\ell'}/m_\ell} \quad , \tag{3.1}$$

where τ_ℓ is the lifetime of the mother lepton ℓ, m_ℓ its mass and $m_{\ell'}$ the mass of the charged daughter lepton. Radiative and higher order corrections have been neglected here. (See also Eq. 2.76). Instead we point out the importance of the so-called low energy parameter η for the muonic decay of τ [113, 41], since $m_\mu/m_\tau \approx 1/17$. With the allowed range of $|\eta_\mu| \leqq 1$ one obtains

$$0.9 < \frac{G_F(\eta_\mu \neq 0)}{G_F(\eta_\mu = 0)} < 1.15 \tag{3.2}$$

if η_μ is not known ! The parameter η_μ can be determined either by analyzing the muon momentum distribution or by deriving upper limits for the coupling constants by measuring the decay parameters ξ'_μ, ξ_μ and δ_μ which will constrain

the value of η_μ.

We note that the parameter η is due to the interference of interactions leading to the same helicities of the leptons in the final state, but to opposite chiralities for the charged leptons μ and e (see Eq. 2.77). Therefore the terms with η in the spectrum or the total decay rate Γ are proportional to the corresponding masses m_μ or m_e. With a dominant left-handed vector interaction a scalar interaction could contribute in *first* order according to

$$\eta \approx \tfrac{1}{2} Re\, g^S_{RR} \quad . \tag{3.3}$$

If we further assume the coupling to be caused by a charged Higgs particle with a strength proportional to the mass of the charged daughter lepton, then we obtain $\eta_\mu/\eta_e = m_\mu/m_e \approx 207$. The sensitivity for this kind of scalar coupling would therefore be $\approx 43\,000$ times larger for the decay of a τ to a μ than for the decay into an electron ! We conclude that the measurement of η_μ is of special interest and note that it should be possible to extract a value from existing data (see Sect. 3.3.2).

3.3. Measurements

The experimental methods used to measure the observables of leptonic τ decays differ from those of μ decay due to several reasons:

a) Muons from $\pi^\pm$ or $K^\pm$ decays are strongly polarized due to the weak interaction causing the meson decay. Decay asymmetry experiments then yield the product of the polarization with the asymmetry parameters. τ leptons, in contrast, used to be produced in pairs of τ^+ and τ^- from colliding e^+ and e^- beams at energies below the Z^0 resonance. The τ's are then unpolarized, being produced via electromagnetic interaction. Their spins, however, are correlated [114] so that the asymmetry parameters can be obtained by measuring correlations between the decay products of the two τ's [41, 113]. Recently τ leptons are also produced from Z^0 decay at the Z^0 resonance. They are polarized due to the Z^0 decay, so that again the product of the asymmetry parameters of both decays can be measured [115].

b) The lifetime of the τ is much shorter than the lifetime of the μ, because the leptonic decay rate is proportional to m_ℓ^5 and because the τ lepton can also decay into hadrons. Except when they are produced at threshold the τ leptons decay therefore in flight due to their short lifetime, and their decay spectra generally are not measured in the rest system. It is therefore not possible, for example, to stop τ's in matter and let their spins precess in a weak magnetic field to measure the decay asymmetry, because they are not polarized and because they decay before stopping.

3.3.1. Spectrum Shape

The Michel parameter ϱ is the only decay parameter measured up to date. Earlier measurements left sufficient room for speculation because ϱ_e looked systematically smaller than ϱ_μ (see Table 3.1).

Table 3.1 Measurements of the two Michel parameters ϱ_e and ϱ_μ from leptonic tau decays. All values are in units of 10^{-3}. When two errors are given, the first is statistical and the second systematic.

Experiment	Ref.	ϱ_e	ϱ_μ
DELCO 79	[116]	720 ± 150	
CLEO 85	[117]	600 ± 130	810 ± 130
MAC 87	[118]	$620 \pm 170 \pm 140$	$890 \pm 140 \pm 80$
CB 89	[119]	$640 \pm 60 \pm 70$	
average		640 ± 60	840 ± 110
ARGUS 90	[120]	$747 \pm 45 \pm 28$	$734 \pm 55 \pm 27$

The latest results [120], however, agree well with $\varrho_e = \varrho_\mu$ and with the standard model value. One of the difficulties in these experiments in contrast to the measurement of ϱ in muon decay is the correct identification of the tau. In the ARGUS experiment this was done by identifying the accompanying tau through the decays $\tau^+ \to \bar{\nu}_\tau \pi^+ \pi^+ \pi^-$ and $\tau^+ \to \bar{\nu}_\tau \pi^+ \pi^+ \pi^- \pi^0$. For the energy spectra in the c.m. system the maximum rate is at the highest energies if radiative corrections

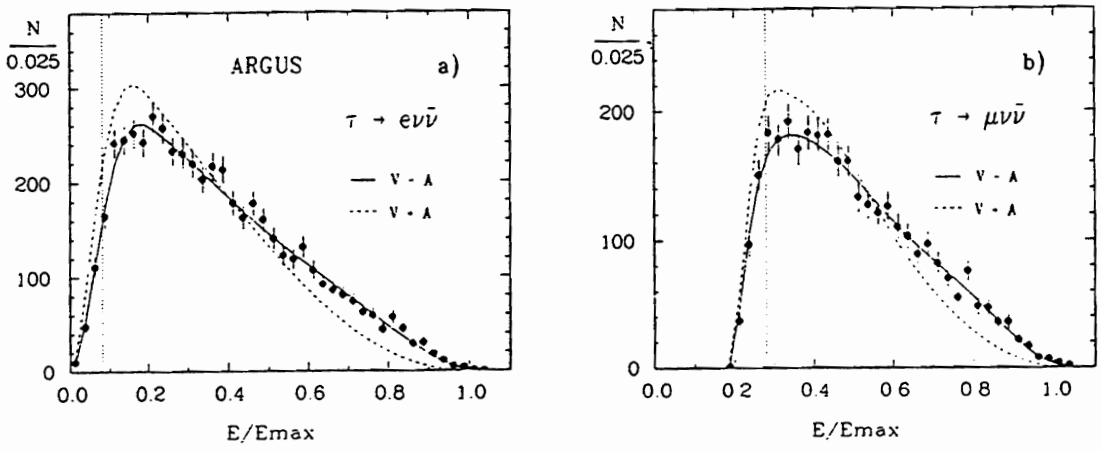

Fig. 3.1 Normalized electron (a) and muon (b) energy distributions for leptonic tau decays show agreement with the standard model and also with a purely right-handed interaction. The dashed curves, labelled "$V+A$", correspond to a coupling $g^V_{LR} = 1$. This has implications for left-right symmetric and for supersymmetric models. See Section 2.3.2 and Table 2.3. From Ref. [120].

are neglected. Due to the Lorentz transformation the maximum in the laboratory system is shifted to lower energies (see Fig. 3.1.).

In the analysis, $\eta = 0$ has been *assumed.* As in μ decay the spectrum depends both on ϱ and η, which are correlated ($\rho_{\varrho\eta} = 0.46$) [41]. Taking this into account would lead to slightly larger errors. On the other hand it has been shown that η_μ can be determined together with the Michel parameter ϱ_μ with a comparable precision because of the favourable mass ratio of m_μ/m_τ. From Eq. 3.1 we see that the measurement of η_μ is essential for a precise test of universality for the muonic τ decay. Implications of ϱ measurements for the Lorentz structure of the interaction are discussed in Sect. 2.3.2 and in Ref. [42]. There exist many four-fermion interactions, including the purely right-handed one with $g^V_{RR} \neq 0$, which lead to $\varrho = 3/4$. See also Table 2.3 and Refs. [17], [78]-[82].

3.3.2. Decay Asymmetry

The four asymmetry parameters ξ_μ, δ_μ, ξ_e and δ_e can be determined by analyzing the decay distributions of spin-correlated τ pairs. It has been shown that the combined measurement of, for example, the e^+ momentum k_e, the μ^- momentum k_μ and the opening angle $\vartheta_{e\mu}$ between the two momenta contains sufficient information not only about η and ϱ but also on the asymmetry parameters ξ and δ [41, 113]. There the figures of merit $\mathcal{M}_i$ were calculated for the decay parameters $x_i = \varrho, \eta, \delta, \xi$ by integration of the distributions $R(k_e, k_\mu, \cos\vartheta_{e\mu})$ and $S(k_e, k_\mu)$ over phase space for 10^7 events. For uncorrelated decay parameters x_i the error Δx_i on the parameter x_i is simply given by $\Delta x_i = \mathcal{M}_i^{-1/2}$. Fig. 3.2 shows the dependence of $\mathcal{M}_i$ on the total energy E_0. Sensitivity is highest for the scalar parameters ϱ_μ and η_μ at threshold, while it increases with energy for the pseudo-scalar parameters δ_μ and ξ_μ. However, measurements are possible for all four quantities both at threshold and at higher energy, e.g. at the Υ resonance.

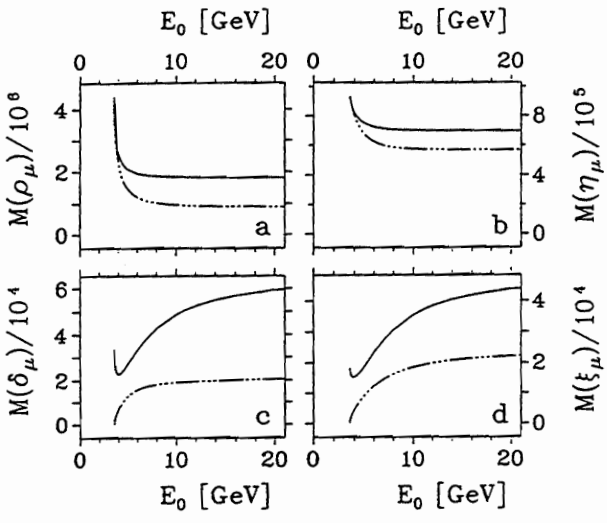

Fig. 3.2 Total Figures of Merit for the leptonic decay parameters $\varrho_\mu, \eta_\mu, \delta_\mu, \xi_\mu$ as a function of the total beam energy E_0. The curves are derived from the correlated distributions $R(k_e, k_\mu, \cos\vartheta_{e\mu})$ (solid lines) and $S(k_e, k_\mu)$ (dashed lines) for the reactions $e^+e^- \rightarrow \tau^+\tau^- \rightarrow (\mu^+\nu_\mu\bar{\nu}_\tau)(e^-\bar{\nu}_e\nu_\tau)$ by numerical integration. From Ref. [41, 113].

In a joint analysis of spin-correlated $\tau^+\tau^-$ pairs decaying into $\mu^\pm, e^\pm, K^\pm$ or $\pi^\pm$ the statistical errors were calculated for an ideal detector [41] taking into account the measured branching ratios. For 10^7 τ pairs produced at a c.m. energy of 10.55 GeV the statistical errors are $\Delta\varrho = 2\times10^{-3}$, $\Delta\eta_\mu = 3\times10^{-3}$, $\Delta\xi = 13\times10^{-3}$ and $\Delta\delta = 11\times10^{-3}$. Instead of evaluating with respect to ξ and δ it is highly recommended to use instead the linear combination Q_R^τ which is the probability of the τ to be right-handed in the decay (see Sect. 2.3.3). Q_R^τ can be determined much more precisely than either ξ or δ alone, because these two parameters are strongly negatively correlated which leads to $\Delta Q_R^\tau = 6.7\times10^{-3}$. Q_R^τ is equal to the sum of the squares of five complex coupling constants (see Eq. 2.72) and supposed to be zero in the standard model so that a precise measurement puts upper limits on each of the coupling constants individually.

3.3.3. Muon Polarization

In muon decay the polarization of positrons from stopped muons is measured by annihilation in flight or Bhabha scattering on longitudinally polarized electrons. The analyzing power is rather large for both processes and can be close to one, but the final measured asymmetry is of the order of a few percent because only every fourteenth electron in the magnetized iron foil is polarized. For the decay $\tau^+ \to \bar{\nu}_\tau\mu^+\nu_\mu$ one can use the decay asymmetry of the stopped μ^+ with the ten-fold higher *effective* analyzing power of 1/3 ! To perform this kind of experiment one needs outside of the main detector a dedicated polarimeter consisting of several alternating planes of nondepolarizing material like aluminium or marble plates, scintillators and an array of drift tubes or proportional chambers to measure the direction of the muons and their decay positrons. The stopped muons would precess in a small magnetic field $B \approx 6\ mT$ which should be tangential to the (assumed) cylindrical surface of the main detector. By measuring the time distribution of the decay one can derive the decay asymmetry and from this the longitudinal polarization of the muon.

Such a measurement has been performed at muon momenta of 16 GeV/c for the reaction $\bar{\nu}_\mu Fe \to X\mu^+$ [121] where the chirality transfer from the $\bar{\nu}_\mu$ onto the μ^+ was measured. There by detecting 3400 events a statistical error on the μ^+ polarization of 20% was reached. Using this result the presumable statistical error which could be reached in a B meson factory for 10^7 produced τ pairs was estimated to 15% [122]. According to Eq. 2.73 this corresponds to an error of 7.5 % for Q_R^μ which is the probability for the μ to be right-handed in τ decay and allows one to put upper limits to $|g_{RR}^S|$, $|g_{RL}^S|$, $|g_{RR}^V|$, $|g_{RL}^V|$ and $|g_{RL}^T|$ simultaneously. With this very important measurement one can get information about three types of interactions not accessible by the asymmetry measurement and put upper limits on any *type* of interaction where the right-handed component of the τ takes part in leptonic τ decays.

References

[1] S.L. Glashow, Nucl. Phys. **22** (1961) 579.

[2] S. Weinberg, Phys. Rev. Lett. **19** (1967) 1264

[3] A. Salam, in *Elementary Particle Theory*, ed. N. Svartholm, (Almquist and Wiksells, Stockholm, 1969), p. 367.

[4] W. Fetscher, H.-J. Gerber and K.F. Johnson, Phys. Lett. **173B** (1986) 102.

[5] L. Michel, Proc. Phys. Soc. **A63** (1950) 514.

[6] F. Scheck, *Lepton, Hadrons and Nuclei* (North-Holland, Amsterdam, 1983).

[7] K. Mursula and F. Scheck, Nucl. Phys. **B253** (1985) 189.

[8] C. Jarlskog, Nucl. Phys. **75**, (1966) 659.

[9] R. Engfer and H.K. Walter, Ann. Rev. Nucl. Part. Sci. **36** (1986) 327.

[10] Martin L. Perl, Rep. Prog. Phys. **55** (1992) 653.

[11] W. Pauli, Nuov. Cim. **6** (1957) 204.

[12] P. Langacker and D. London, Phys. Rev. **D 39** (1989) 266.

[13] Particle Data Group, K. Hikasa *et al.*, Phys. Rev. **D 45** (1 June 1992).

[14] K. Jungmann, V.W. Hughes and G. zu Putlitz (Eds.), *The Future of Muon Physics* (Springer-Verlag, Berlin Heidelberg New York,1992);
Z. Phys. **C56** (1992) 1.

[15] F. Scheck, *Muon Physics*, Phys. Rep. **44** (1978).

[16] P. Langacker, Comments Nucl. Part. Phys. **19** (1989) 1.

[17] P. Herczeg, Phys. Rev. **D 34** (1986) 3449.

[18] *International Colloquium on the History of Particle Physics* , Journal de Physique **43** (1982).

[19] M. Fierz, Z. Physik **101** (1937) 553.

[20] T. Kinoshita and A. Sirlin, Phys. Rev. **108** (1957) 844.

[21] W. Fetscher and H.-J. Gerber, in Particle Data Group, K. Hikasa *et al.*, Phys. Rev. **D 45**, (1 June 1992) VI.16.

[22] Wulf Fetscher, Phys. Rev. Lett. **69** (1992) 2758.

[23] Wulf Fetscher, submitted for publication (January, 1993)

[24] M. Jonker *et al.* (CHARM I collaboration), Phys. Lett. **93 B** (1980) 203; F. Bergsma *et al.* (CHARM I collaboration), Phys. Lett. **122 B** (1983) 465.

[25] K. Mursula, M. Roos and F. Scheck, Nucl. Phys. **B219** (1983) 321.

[26] W. Fetscher, in *Neutrino 86: Neutrino Physics and Astrophysics*, proceedings of the 12th International Conference, Sendai, Japan, 1986, edited by T. Kitagaki and H. Juta (World Scientific, Singapore, 1986).

[27] W. Fetscher, Phys. Lett. **140B** (1984) 117.

[28] B. Balke *et al.*, Phys. Rev. **D 37** (1988) 587.

[29] W. Eichenberger, R. Engfer and A. van der Schaaf, Nucl. Phys. **A412** (1984) 523.

[30] R.H. Pratt, Phys. Rev. **111**, (1958) 649.

[31] A. Kersch, N. Kraus and R. Engfer , Nucl. Phys. **A485** (1988) 523.

[32] H. Burkard *et al.*, Phys. Lett. **160 B** (1985) 343.

[33] S.E. Derenzo, Phys. Rev. **181**, (1969) 1854.

[34] H. Burkard *et al.*, Phys. Lett. **150 B** (1985) 242.

[35] I. Beltrami *et al.*, Phys. Lett. **194 B** (1987) 326.

[36] A. Jodidio *et al.*, Phys. Rev. **D 34** (1986) 1967; A. Jodidio *et al.*, Phys. Rev. **D 37** (1988) 237.

[37] J. Imazato *et al.*, Phys. Rev. Lett. **69** (1992) 877.

[38] B. Bodmann *et al.* (KARMEN collaboration), Phys. Lett. **280 B** (1992) 198.

[39] D. Geiregat *et al.* (CHARM II collaboration), Phys. Lett. **247B**, (1990) 131.

[40] S. R. Mishra *et al.* (CCFR collaboration), Phys. Lett. **252B** (1990) 170.

[41] Wulf Fetscher, Phys. Rev. **D 42**, (1990) 1544.

[42] H.-J. Gerber, "Lepton Properties", Proceedings International Europhysics Conference on High Energy Physics, Uppsala 1987. Olga Botner (Ed.), Uppsala University.

[85] H. Haber and G. Kane, Phys. Rep. **117** (1985) 75.

[86] H.A. Tolhoek, Rev. Mod. Phys. **28** (1956) 277.

[87] L.A. Page, Rev. Mod. Phys. **31** (1959) 759.

[88] H. Frauenfelder and A. Rossi, *Determination of the Polarization of Electrons and Photons*, in "Nuclear Physics", L.C.L. Yuan and C.S. Wu (ed.), (Academic Press, N.Y. 1963).

[89] A. Ashkin, L.A. Page and W.M. Woodward, Phys. Rev. **94** (1954) 357.

[90] L.A. Page, Phys. Rev. **106** (1957) 394.

[91] W.H. McMaster, Nuov. Cim. **17** (1960) 395.

[92] A.M. Bincer, Phys. Rev. **107** (1957) 1434.

[93] K. Bockmann, G. Kramer and W.R. Theis, Z. Phys. **150** (1958) 201.

[94] J. Ullman, H. Frauenfelder, H.J. Lipkin and A. Rossi, Phys. Rev. **122** (1961) 963.

[95] Lester L. DeRaad, Jr. and Yee Jack Ng, Phys. Rev. **D 11** (1975) 1586.

[96] W.E. Fischer and F. Scheck, Nucl. Phys. **B83** (1974) 25.

[97] M.T. Mehr and F. Scheck, Nucl. Phys. **B149** (1979) 123.

[98] A. Bühler, N. Cabibbo, M. Fidecaro, T. Massam, Th. Müller, M. Schneegans and A. Zichichi, Phys. Lett. **7** (1963) 368.

[99] S. Bloom, L.A. Dick, L. Feuvrais, G.R. Henry, P.C. Macq and M. Spighel, Phys. Lett. **8** (1964) 87.

[100] J. Duclos, J. Heintze, A. de Rújula and V. Soergel, Phys. Lett. **9** (1964) 62.

[101] Daniel M. Schwartz, Phys. Rev. **162** (1967) 1306.

[102] G.G. Scott, Rev. Mod. Phys. **34** (1962) 102.

[103] James S. Barber and Robert S. Shrock, Phys. Lett. **139B** (1984) 427.

[104] S.L. Adler, Phys. Rev. **B 135** (1964) 963.

[105] A. van der Schaaf, R. Engfer, H.P. Povel, W. Dey, H.K. Walter and C. Petitjean, Nucl. Phys. **A340**, (1980) 249.

[106] B.C. Barish and R. Stroynowski, Phys. Rep. **157** (1988) 1.

[107] K.K. Gan and M.L. Perl, Int. J. Mod. Phys. **A3** (1988) 531.

[108] T.D. Lee and C.N. Yang, Phys. Rev. **108**, (1957) 1611.

[109] J. Missimer, F. Scheck and R. Tegen, Nucl. Phys. **B188** (1981) 29

[110] H. Albrecht *et al.* (ARGUS collaboration), Phys. Lett. **202B** (1988) 149.

[111] H. Albrecht *et al.* (ARGUS collaboration), Phys. Lett. **292B** (1992) 221.

[112] J.Z. Bai *et al.* (BES collaboration), Phys. Rev. Lett. **69** (1992) 3021.

[113] W. Fetscher, *Leptonic τ Lepton Decays*, in *Proposal for a B-Meson-Factory*, PSI Report **PR-88-09** (1988).

[114] Y.S. Tsai, Phys. Rev. **D 4**, (1971) 2821.

[115] C.A. Nelson, Phys. Rev. **D 40**, (1989) 123.

[116] W. Bacino *et al.* (DELCO collaboration), Phys. Rev. Lett. **42**, (1979) 749.

[117] S. Behrends *et al.* (CLEO collaboration), Phys. Rev. **D 32**, (1985) 2468.

[118] W.T. Ford *et al.* (MAC collaboration), Phys. Rev. **D 36**, (1987) 1971.

[119] H. Janssen *et al.* (Crystal Ball collaboration), Phys. Lett. **228B**, (1989) 273.

[120] H. Albrecht *et al.* (ARGUS collaboration), Phys. Lett. **246B**, (1990) 278.

[121] M. Jonker *et al.* (CHARM I collaboration), Phys. Lett. **86B**, (1979) 229.

[122] K. Wacker *et al.*, *Proposal for a B-Meson-Factory*, PSI Report **PR-88-09** (1988).